Robust structural feedback linearization based on the nonlinearities rejection

Moisés E. Bonilla, Luis Angel Blas, Vadim Azhmyakov, Michel Malabre,
Sergio Salazar

HAL Id: hal-02362693

https://hal.science/hal-02362693v2

Submitted on 21 Nov 2019

Journal of the Franklin Institute

Robust Structural Feedback Linearization Based on the Nonlinearities Rejection
--Manuscript Draft--

Robust Structural Feedback Linearization Based on the Nonlinearities Rejection

M. Bonilla[a,*], L.A. Blas[a,b], V. Azhmyakov[c], M. Malabre[d], S. Salazar[e]

[a] *Control Automático, CINVESTAV-CNRS IPN, CDMX, México*
[b] *Ph.D. Student, sponsored by CONACyT, México*
[c] *Department of Mathematical Sciences, Universidad EAFIT, Medellin, Republic of Colombia*
[d] *CNRS, LS2N, UMR 6004, Nantes, France*
[e] *Sistemas Autónomos de Navegación Aérea y Submarina, CINVESTAV-CNRS IPN, CDMX, México*

Abstract

In this paper, we consider a class of affine control systems and propose a new structural feedback linearization technique. This relatively simple approach involves a generic linear-type control scheme and follows the classic failure detection methodology. The robust linearization idea proposed in this contribution makes it possible an effective rejection of nonlinearities that belong to a specific class of functions. The nonlinearities under consideration are interpreted here as specific signals that affect the initially given systems dynamics. The implementability and efficiency of the proposed robust control methodology is illustrated via the attitude control of a Planar Vertical Take Off Landing (PV-TOL) system.

Keywords: nonlinear dynamic systems, non-standard feedback linearization, nonlinearities rejection, failure reconstruction.

Notation. The following notation is used through this paper.

- Script capitals $\mathscr{V}$, $\mathscr{W}$, ... denote finite dimensional linear spaces with elements v, w, ... The expression $\mathscr{V} \approx \mathscr{W}$ stands for $\dim(\mathscr{V}) = \dim(\mathscr{W})$. Moreover, when $\mathscr{V} \subset \mathscr{W}$, $\frac{\mathscr{W}}{\mathscr{V}}$ or $\mathscr{W}/\mathscr{V}$ stands for the quotient space $\mathscr{W}$ modulo $\mathscr{V}$. Next, $\mathscr{V}^\kappa$ denotes the Cartesian product $\mathscr{V} \times \cdots \times \mathscr{V}$ (κ times). By $X : \mathscr{V} \to \mathscr{W}$, we denote a linear transformation operating from $\mathscr{V}$ to $\mathscr{W}$. As usually, $\operatorname{Im} X = X\mathscr{V}$ denotes the image of X and $\ker X$ is its kernel. Moreover, $X^{-1}\mathscr{T}$ stands for the inverse image of $\mathscr{T} \subset \mathscr{W}$. The special subspaces $\operatorname{Im} B$ and $\ker C$ are denoted by $\mathscr{B}$, and $\mathscr{K}$, respectively. The zero dimension subspace is indicated as 0 and $\sigma\{A\}$ denotes the spectrum of the linear transformation A. The identity operator is denoted by I: I$x = x$; A^0 is the identity operator, for any given linear transformation A. The matrix of a given linear transformation $A : \mathscr{X} \to \mathscr{X}$ in a given basis is noted as $\mathbf{A} \in \mathbb{R}^{n \times n}$. Additionally, for the elements v, w, ... $\in$

$\mathscr{X}$ in the given basis, we use the notation $\mathbf{v}$, $\mathbf{w}$, $\ldots \in \mathbb{R}^n$. In our paper, $\mathbf{1}$ stands for the vector where all its components are equal to 1 and BD $\{\mathbf{X}_1, \ldots, \mathbf{X}_k\}$ denotes a block diagonal matrix.

$\mathcal{C}_{(M, S)}$ denotes the controllability map of the pair (M, S), $M : \mathscr{X} \to \mathscr{X}$ and $S : \mathscr{Q} \to \mathscr{X}$, namely:

$$\mathcal{C}_{(M, S)} = \begin{bmatrix} S & M\,S & \cdots & M^{(n-1)}\,S \end{bmatrix}$$

and we denote: $\langle A \mid \mathscr{B} \rangle = \operatorname{Im} \mathcal{C}_{(A, B)}$. We also introduce:

$$\mathcal{C}^{[\bar{n}]}_{(M, S)} = \begin{bmatrix} S & M\,S & \cdots & M^{(\bar{n}-1)}\,S \end{bmatrix}.$$

The unobservable subspace of the pair (C, M), $C : \mathscr{X} \to \mathscr{Y}$ and $M : \mathscr{X} \to \mathscr{X}$ is denoted by $\langle \mathscr{K} \mid M \rangle$.

- $\mathrm{d}^0/\mathrm{d}t^0$ stands for the identity operator: $\mathrm{d}^0 v/\mathrm{d}t^0 = v$. $\Psi_n(\mathrm{d}/\mathrm{d}t)$ stands for the differential operator (from $\mathscr{Q}$ to $\mathscr{Q}^n$):

$$\Psi_n(\mathrm{d}/\mathrm{d}t) = \begin{bmatrix} \mathrm{I} & \mathrm{I}\,\mathrm{d}/\mathrm{d}t & \cdots & \mathrm{I}\,\mathrm{d}^{n-1}/\mathrm{d}t^{n-1} \end{bmatrix}^T.$$

- Given a vector $\mathbf{x} \in \mathbb{R}^n$, the expression $\|\mathbf{x}\|$ means the Euclidean norm and $\mathcal{B}_\rho$ stands for a specific neighborhood with a radius ρ:

$$\mathcal{B}_\rho = \{\, \mathbf{x} \in \mathbb{R}^n : \|\mathbf{x}\| < \rho \,\}.$$

Similarly to the above notation, $\|\mathbf{x}\|_\infty$ is the usual *sup*-norm and $\mathcal{C}^\infty$ denotes the set of infinitely differentiable functions.

- We next define the matrix $A_{c_n} \in \mathbb{R}^{n \times n}$, and the vectors $\chi_n^i \in \mathbb{R}^{n \times 1}$, $i \in \{1, \ldots, n\}$, as follows:

$$A_{c_n} \triangleq \begin{bmatrix} 0 & 1 & 0 & \cdots & 0 & 0 \\ \cdot & \cdot & \cdot & \cdots & \cdot & \cdot \\ 0 & 0 & 0 & \cdots & 0 & 1 \\ 0 & 0 & 0 & \cdots & 0 & 0 \end{bmatrix}, \chi_n^1 \triangleq \begin{bmatrix} 1 \\ 0 \\ \vdots \\ 0 \end{bmatrix}, \chi_n^2 \triangleq \begin{bmatrix} 0 \\ 1 \\ 0 \\ \vdots \\ 0 \end{bmatrix}, \cdots, \chi_n^n \triangleq \begin{bmatrix} 0 \\ \vdots \\ 0 \\ 1 \end{bmatrix}$$

$$(1)$$

1. Introduction and Motivation

Linearization techniques have been established for a long-time as a powerful tool for simplified analysis and design of general nonlinear dynamic systems. "Linearize" the initial nonlinear problem has various meanings in Applied Mathematics, depending on the areas where it is defined, depending also on what one linearizes (a functional, an equation *etc.*). In the context of a robust control design, when dealing with the practical stabilization of the initially given nonlinear dynamic model, the most common way of looking at linearization is to consider a suitable version of the so called feedback linearization [21]. The initial

concept of feedback linearization was introduced by [21, 35]. The linearization techniques constitute nowadays a crucial tool of the modern Control Theory and are widely used in various engineering applications.

Recall that a general idea for linearization based on the choice of a different state representation has been established since the work of [21] and [29]. This pioneering technique is in some sense similar to a specific choice of references or suitable coordinate systems in Lagrange mechanics. Roughly speaking, the conventional feedback linearization constitutes an equivalent transformation of the original system models into equivalent dynamic models. This resulting model is a simpler one and possesses some useful behavioral properties. In modern engineering, there are many applications of the various feedback linearization approaches. These applications are devoted (but not restricted) to the helicopters flight dynamics, high-performance aircraft control, industrial robots behavior design, biomedical devices and intelligent vehicles control [26, 25, 14, 31, 38, 30, 42].

Also notice that the main idea of the classic feedback linearization is associated in fact with an algebraic transformation of the initially given nonlinear system (see *e.g.* [35, 21, 28, 20]. Evidently, a general linearization benefits the engineering analysis and design from the possibility to apply the well-established techniques of the Linear Control Theory. Consider the following (nonlinear) control-affine system:

$$\begin{array}{rcl} \frac{\mathrm{d}}{\mathrm{d}t}x(t) & = & f(x(t)) + g(x(t))u(t), \\ y(t) & = & Cx(t), \end{array} \tag{1.1}$$

where $x \in \mathbb{R}^n$ denotes the state variable, $y \in \mathbb{R}^p$ is an output and $u \in \mathbb{R}^m$ is the control input. Here $p \leq m$, $f(x)$ and $g(x)$ are analytic vector fields on $\mathbb{R}^n$ and $C \in \mathbb{R}^{p \times n}$. We now make some technical assumptions that guarantee existence and uniqueness of a local solution to the initial system (1.1).

H1. *The origin $x_o = 0 \in \mathbb{R}^n$ is an equilibrium point of the autonomous system (1.1) ($u = 0$). That means $f(0) = 0$.*

H2. *The given functions f and g are continuously infinitely differentiable in a neighborhood of the equilibrium point 0.*

From the above assumptions also follows the existence of positive constants r_ℓ, $K_{\mathcal{L}_f}$ and $K_{\mathcal{L}_g}$ such that $\|f(x_1) - f(x_2)\| \leq K_{\mathcal{L}_f} \|x_1 - x_2\|$, and $\|g(x_1) - g(x_2)\| \leq K_{\mathcal{L}_g} \|x_1 - x_2\|$ for all x_1, $x_2 \in \mathcal{B}_{r_\ell}$. Note that from **H1** also follows the existence of some positive constants h_f and h_g such that $\|f(0)\| \leq h_f$ and $\|g(0)\| \leq h_g$ for all $t \geq 0$. We refer to [39] for the necessary proofs and corresponding analytical details.

In order to have a wide panorama of this paper, a short overview related to some existing (classic) linearization techniques is now given, as well as the principal ideas issued in this contribution. For this, an academic example is introduced, which will be used all along this paper.

Example 1. *(Academic Example) The PVTOL (Planar Vertical Take off Landing) System of Fig. 1. The PVTOL is one to the most simple (theoretical) aircraft vehicles, which is very close to a (real) Quadrotor Laboratory Prototype. Here m_T is the total mass, J is the moment of inertia with respect to the rotation axis oy and L denotes the distance from the center of gravity to the thrusters. The motion is considered with respect to a fixed orthogonal axis set $(o\mathsf{xyz})$, where $o\mathsf{z}$ points vertically down along the gravity vector $\begin{bmatrix} 0 & 0 & g \end{bmatrix}^T$. The origin o is located at the desired height $\bar{\mathsf{z}}$ to the ground level. Moreover, θ denotes here the Euler angle determined by the axis $o_B\mathsf{y}_B$. Here $(o_B\mathsf{x}_B\mathsf{y}_B\mathsf{z}_B)$ is the body axis system with its origin in o_B (fixed at the centre of gravity of the PVTOL). The PVTOL moves in the plane $(o\mathsf{xz})$. By $\mathfrak{f}_1, \mathfrak{f}_2 \in \begin{bmatrix} 0, mg \end{pmatrix}$ we denote the actuators (thrusters).*

Figure 1: Schematic PVTOL diagram

The mathematical model of the PVTOL system is represented by the following (behavioral) equations. We refer to [15, 11]) for the analytical details.

$$\begin{bmatrix} \mathrm{d}^2\mathsf{x}/\mathrm{d}t^2 \\ \mathrm{d}^2\theta/\mathrm{d}t^2 \\ \mathrm{d}^2\mathsf{z}/\mathrm{d}t^2 \end{bmatrix} = \begin{bmatrix} (1/m_T)\, u_{\mathsf{z}} \tan(\theta) \\ (L/J)\, u_{\mathsf{x}} \\ (1/m_T)\, u_{\mathsf{z}} + g \end{bmatrix}. \qquad (1.2)$$
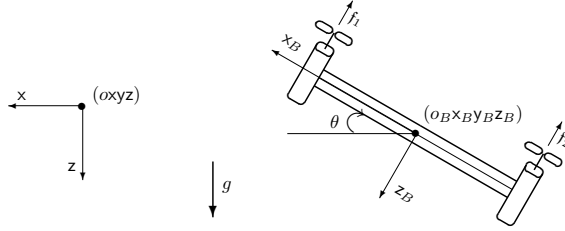
Here:

$$u_{\mathsf{z}} = -(\mathfrak{f}_1 + \mathfrak{f}_2)\cos\theta \quad and \quad u_{\mathsf{x}} = (\mathfrak{f}_1 - \mathfrak{f}_2).$$

The output and the state variables of the above model can be interpreted as follows:

$$y \;\dot{=}\; \mathsf{x},$$
$$x \;\dot{=}\; \begin{bmatrix} \mathsf{x} & \mathrm{d}\mathsf{x}/\mathrm{d}t & \theta & \mathrm{d}\theta/\mathrm{d}t & \mathsf{z} & \mathrm{d}\mathsf{z}/\mathrm{d}t \end{bmatrix}^T.$$

Applying the conventional gravity compensation control law:

$$u_{\mathsf{z}} = m_T \left(\begin{bmatrix} 0 & 0 & 0 & 0 & -a_{\mathsf{z},2} & -a_{\mathsf{z},1} \end{bmatrix} x - g \right) \quad and \quad u \,\dot{=}\, (L/J)\, u_{\mathsf{x}}, \qquad (1.3)$$

the z-dynamics is represented by the differential equation:

$$\left(\mathrm{d}^2/\mathrm{d}t^2 + a_{\mathsf{z},1}\,\mathrm{d}/\mathrm{d}t + a_{\mathsf{z},2} \right) \mathsf{z}(t) = 0,$$

4

where $\pi_{\mathsf{z}}(\mathsf{s}) = \mathsf{s}^2 + a_{\mathsf{z},1}\mathsf{s} + a_{\mathsf{z},2}$ is a Hurwitz polynomial. Finally we deduce the nonlinear state description (cf. (1.1))

$$\frac{\mathrm{d}}{\mathrm{d}t}x \;=\; \underbrace{\begin{bmatrix} x_2 \\ -(g + a_{\mathsf{z},2}x_5 + a_{\mathsf{z},1}x_6)\tan(x_3) \\ x_4 \\ 0 \\ x_6 \\ -(a_{\mathsf{z},2}x_5 + a_{\mathsf{z},1}x_6) \end{bmatrix}}_{\mathbf{f}(x)} + \underbrace{\begin{bmatrix} 0 \\ 0 \\ 0 \\ 1 \\ 0 \\ 0 \end{bmatrix}}_{\mathbf{g}(x)} u,$$

$$y \;=\; \underbrace{\begin{bmatrix} 1 & 0 & 0 & 0 & 0 & 0 \end{bmatrix}x}_{h(x)}. \qquad (1.4)$$

1.1. An Approximated Input-Output Linearization

One of the classic linearization techniques (widely used by "pioneers" of the modern Control Theory) consists in representation of (1.1) in the form of Taylor's series around the equilibrium point $x_o = 0 \in \mathbb{R}^n$ and in the corresponding approximation using the first order terms. Applying this simple idea we get:

$$\begin{aligned} \frac{\mathrm{d}}{\mathrm{d}t}x(t) &= A\,x(t) + B\,u(t) + f_o(x(t),\,u(t))\,, \\ y(t) &= C\,x(t)\,, \end{aligned} \qquad (1.5)$$

where

$$A \doteq [\partial f/\partial x]_{x=0} \in \mathbb{R}^{n\times n}\,, \quad B \doteq [g]_{x=0} \in \mathbb{R}^{n\times m}\,, \qquad (1.6)$$

and $x \in \mathscr{X} \approx \mathbb{R}^n$ is the state, $u \in \mathscr{U} \approx \mathbb{R}^m$ is the input, $y \in \mathscr{Y} \approx \mathbb{R}^p$ is the output. Moreover, we have:

$$\begin{aligned} f_o(x(t),\,u(t)) &= \Delta f(x(t)) + \Delta g(x(t))u(t)\,, \\ \Delta f(x(t)) &= f(x(t)) - Ax(t)\,, \\ \Delta g(x(t)) &= g(x(t)) - B\,. \end{aligned} \qquad (1.7)$$

From the above formalism we can deduce that for a sufficiently small neighborhood $\mathcal{B}_\rho$: $|\Delta f(x(t))| \to 0$ and $|\Delta g| \to 0$, the resulting obtained linear state approximation (for all $x_\ell \in \mathcal{B}_\rho$) can then be written as follows:

$$\begin{aligned} \frac{\mathrm{d}}{\mathrm{d}t}x_\ell(t) &= A\,x_\ell(t) + B\,u(t)\,, \\ y(t) &= C\,x_\ell(t)\,, \end{aligned} \qquad (1.8)$$

This classical linearization technique is a formal consequence of the celebrated Stability Principle of the First Approximation (SPFA). Recall that this principle states that the existence of a state feedback, $F_{st} \in \mathbb{R}^n$, which stabilizes the linear state approximation (1.8), implies the required stability property of (1.5) (by F_{st}) in the neighborhood $\mathcal{B}_\rho$. We refer to [22], [39], [23], [35], [33] for the corresponding technical details.

For the academic example (1.4), the matrices A, B and C of (1.8) are (*cf.* (1.6)):

$$A = \left[\begin{array}{c|c} A_{0,\mathsf{x}} & 0 \\ \hline 0 & A_{\mathsf{z}} \end{array}\right], \quad B = \left[\begin{array}{c} B_{\mathsf{x}} \\ \hline 0 \end{array}\right], \quad C = \left[\ C_{\mathsf{x}} \mid 0\ \right], \tag{1.9}$$

where:

$$A_{0,\mathsf{x}} = \begin{bmatrix} 0 & 1 & 0 & 0 \\ 0 & 0 & -g & 0 \\ 0 & 0 & 0 & 1 \\ 0 & 0 & 0 & 0 \end{bmatrix}, \quad \left\{\begin{array}{l} A_{\mathsf{z}} = \overline{A}_{\mathsf{z}} + B_{\mathsf{z}}\,F_{\mathsf{z}}, \quad F_{\mathsf{z}} = \left[\ -a_{\mathsf{z},2} \quad -a_{\mathsf{z},1}\ \right], \\ B_{\mathsf{x}} = \chi_4^4\,, \ C_{\mathsf{x}} = (\chi_4^1)^T\,, \ \overline{A}_{\mathsf{z}} = A_{c_2}\,, \ B_{\mathsf{z}} = \chi_2^2\,. \end{array}\right.$$
$$\tag{1.10}$$

Moreover, we have $x = \left[\ x_{\mathsf{x}} \quad x_{\mathsf{z}}\ \right]^T$, $x_{\mathsf{x}} = \left[\ \mathsf{x} \quad d\mathsf{x}/dt \quad \theta \quad d\theta/dt\ \right]^T$, $x_{\mathsf{z}} = \left[\ \mathsf{z} \quad d\mathsf{z}/dt\ \right]^T$.

We next apply the stabilizing state feedback:

$$u = F_{\mathsf{x}}\,x_{\mathsf{x}} + \bar{u}_{\mathsf{x}}, \quad \text{where:}\ \ F_{\mathsf{x}} = \left[\ a_{\mathsf{x},4}/g \quad a_{\mathsf{x},3}/g \quad -a_{\mathsf{x},2} \quad -a_{\mathsf{x},1}\ \right]. \tag{1.11}$$

Note that the characteristic polynomial of the closed loop matrix,

$$A_{\mathsf{x}} = A_{0,\mathsf{x}} + B_{\mathsf{x}}\,F_{\mathsf{x}}\,, \tag{1.12}$$

is the Hurwitz polynomial:

$$\pi_{x_{\mathsf{x}}}(\mathsf{s}) = \det(\mathsf{s}I - A_{\mathsf{x}}) = \mathsf{s}^4 + a_{\mathsf{x},1}\mathsf{s}^3 + a_{\mathsf{x},2}\mathsf{s}^2 + a_{\mathsf{x},3}\mathsf{s} + a_{\mathsf{x},4}\,. \tag{1.13}$$

The state space description of the obtained closed loop system can be expressed as:

$$\begin{aligned} \frac{d}{dt}x &= \left[\begin{array}{c|c} A_{\mathsf{x}} & 0 \\ \hline 0 & A_{\mathsf{z}} \end{array}\right]x + \left[\begin{array}{c} B_{\mathsf{x}} \\ \hline 0 \end{array}\right]\bar{u}_{\mathsf{x}} + \left[\begin{array}{c} S_{\mathsf{x}} \\ \hline 0 \end{array}\right]q_{\mathsf{x}}(x)\,, \\ \mathsf{x} &= \left[\ C_{\mathsf{x}} \mid 0\ \right]x\,. \end{aligned} \tag{1.14}$$

Here:

$$\begin{aligned} S_{\mathsf{x}} &= \chi_4^2\,, \\ q_{\mathsf{x}}(x) &= -\,(a_{\mathsf{z},2}x_5 + a_{\mathsf{z},1}x_6)\tan(x_3) + g\,(x_3 - \tan(x_3)) = d^2\mathsf{x}/dt^2 + g\,\theta\,. \end{aligned} \tag{1.15}$$

1.2. An Exact Input-Output Linearization

The next linearization technique we examine here is the so called *"exact input output linearization"*. Consider the basic hypothesis **H1**, **H2** and additionally make the following non-restrictive assumption.

H 3. *The dynamic system under consideration has relative degree*[1] *n at any point in $\mathbb{R}^n$*

---
[1] For the definition of relative degree see [21] and [23].

Taking into consideration the above assumptions, the conventional feedback linearization can effectively be applied to the initial system (1.1) (see *e.g.* [21], [23] and [35]). Let us briefly examine the input-output linearization technique for the specific case:

$$p = m = 1.$$

From **H3** it follows that there exists a specific diffeomorphism $T_{dif} : \mathbb{R}^n \to \mathbb{R}^n$, $\xi(t) = T_{dif}(x(t))$ such that:

$$
\begin{aligned}
\tfrac{\mathrm{d}}{\mathrm{d}t}\xi(t) &= A_{c_n}\,\xi(t) + \chi_n^n\left(\alpha(x) + \beta(x)u(t)\right), \\
y(t) &= \left(\chi_n^1\right)^T \xi(t).
\end{aligned}
\tag{1.16}
$$

Here $\xi := \begin{bmatrix} \xi_1 & \cdots & \xi_n \end{bmatrix}^T$.

To get an explicit linearization control law, the additional hypothesis is added.

H 4. *There exits a known positive constant $\bar{\beta}$ such that for all x we have $0 < \bar{\beta} < \beta(x)$.*

Taking into consideration the complete knowledge of the system's parameters and applying the ideal control law:

$$u(t) = \beta^{-1}(x)\left(-\alpha(x) + F_n\,\xi(t)\right), \quad F_n = \begin{bmatrix} -a_n & \cdots & -a_1 \end{bmatrix} \tag{1.17}$$

we obtain the resulting linear closed loop system

$$
\begin{aligned}
\tfrac{\mathrm{d}}{\mathrm{d}t}\xi(t) &= \left(A_{c_n} + \chi_n^n\,F_n\right)\xi(t), \\
y(t) &= \left(\chi_n^1\right)^T \xi(t).
\end{aligned}
\tag{1.18}
$$

Here $\pi_n(\mathrm{s}) = \mathrm{s}^n + a_1\,\mathrm{s}^{n-1} + \cdots + a_n$ is a Hurwitz polynomial.

We now apply the exact input-output linearization technique to the academic example (1.4). Differentiating the output and taking into consideration the corresponding relative degree, we observe that:

$$
\begin{aligned}
\tfrac{\mathrm{d}}{\mathrm{d}t}\xi &= \left[\begin{array}{c|c} A_{c_4} & 0 \\ \hline 0 & \bar{A}_{\mathsf{z}} \end{array}\right]\xi + \left[\begin{array}{c} B_{\mathsf{x}} \\ \hline 0 \end{array}\right]\left(\alpha(x) + \beta(x)u\right), \\
y &= \begin{bmatrix} C_{\mathsf{x}} & 0 \end{bmatrix}\xi.
\end{aligned}
\tag{1.19}
$$

We use here the additional notation:

$$\xi = \begin{bmatrix} \xi_{\mathsf{x}}^T & x_{\mathsf{z}}^T \end{bmatrix}^T, \quad \xi_{\mathsf{x}} = \begin{bmatrix} \mathsf{x} & \mathrm{d}\mathsf{x}/\mathrm{d}t & \mathrm{d}^2\mathsf{x}/\mathrm{d}t^2 & \mathrm{d}^3\mathsf{x}/\mathrm{d}t^3 \end{bmatrix}^T,$$

$$
\begin{aligned}
\mathrm{d}^2\mathsf{x}/\mathrm{d}t^2 = \mathrm{L}_{\mathbf{f}}^2(h) &= -(g + a_{\mathsf{z},2}\mathsf{z} + a_{\mathsf{z},1}\mathrm{d}\mathsf{z}/\mathrm{d}t)\tan(\theta), \\
\mathrm{d}^3\mathsf{x}/\mathrm{d}t^3 = \mathrm{L}_{\mathbf{f}}^3(h) &= -\mathrm{d}\theta/\mathrm{d}t\,(g + a_{\mathsf{z},2}\mathsf{z} + a_{\mathsf{z},1}\mathrm{d}\mathsf{z}/\mathrm{d}t)\sec^2(\theta) \\
&\quad + \left(a_{\mathsf{z},1}a_{\mathsf{z},2}\mathsf{z} + (a_{\mathsf{z},1}^2 - a_{\mathsf{z},2})\mathrm{d}\mathsf{z}/\mathrm{d}t\right)\tan(\theta),
\end{aligned}
\tag{1.20}
$$

$$
\begin{aligned}
\alpha(x) = \ & \mathrm{L}_{\mathbf{f}}^4(h) = \mathrm{d}\theta/\mathrm{d}t\big(-2\,\mathrm{d}\theta/\mathrm{d}t\,(g + a_{\mathsf{z},_2}\mathsf{z} + a_{\mathsf{z},_1}\mathrm{d}\mathsf{z}/\mathrm{d}t)\tan(\theta) + a_{\mathsf{z},_1}a_{\mathsf{z},_2}\mathsf{z} \\
& +(a_{\mathsf{z},_1}^2 - a_{\mathsf{z},_2})\,\mathrm{d}\mathsf{z}/\mathrm{d}t)\sec^2(\theta) + a_{\mathsf{z},_2}\mathrm{d}\mathsf{z}/\mathrm{d}t\big(-\mathrm{d}\theta/\mathrm{d}t\,\sec^2(\theta) + a_{\mathsf{z},_1}\tan(\theta)\big) \\
& -(a_{\mathsf{z},_2}\mathsf{z} + a_{\mathsf{z},_1}\mathrm{d}\mathsf{z}/\mathrm{d}t)\big(-a_{\mathsf{z},_1}\mathrm{d}\theta/\mathrm{d}t\,\sec^2(\theta) + (a_{\mathsf{z},_1}^2 - a_{\mathsf{z},_2})\tan(\theta)\big), \\
\beta(x) = \ & \mathrm{L}_{\mathbf{g}}^1(\mathrm{L}_{\mathbf{f}}^3(h)) = -(g + a_{\mathsf{z},_2}\mathsf{z} + a_{\mathsf{z},_1}\mathrm{d}\mathsf{z}/\mathrm{d}t)\sec^2(\theta).
\end{aligned}
$$

$$(1.21)$$

Implementing the stabilizing state feedback (*cf.* (1.17)) $u = \beta^{-1}(x)\big(-\alpha(x) + F_4\,\xi + \bar{u}_\mathsf{x}\big)$, $F_4 = \begin{bmatrix} -a_{\mathsf{x},_4} & -a_{\mathsf{x},_3} & -a_{\mathsf{x},_2} & -a_{\mathsf{x},_1} \end{bmatrix}$, we finally get the closed loop state space description:

$$
\begin{aligned}
\frac{\mathrm{d}}{\mathrm{d}t}\xi &= \left[\begin{array}{c|c} A_{c_4 F_4} & 0 \\ \hline 0 & A_\mathsf{z} \end{array}\right]\xi + \left[\begin{array}{c} B_\mathsf{x} \\ \hline 0 \end{array}\right]\bar{u}_\mathsf{x}, \\
\mathsf{x} &= \begin{bmatrix} C_\mathsf{x} & | & 0 \end{bmatrix}\xi.
\end{aligned}
$$

$$(1.22)$$

Note that the characteristic polynomial of the closed loop matrix $A_{c_4\,F_4} = A_{c_4} + B_\mathsf{x}\,F_4$ is the Hurwitz polynomial (1.13).

1.3. Exact Structural Linearization

With the help of the academic example (1.4), we now introduce an exact linearization technique based on the system structure. For this, we first apply the change of variable:[2]

$$
\zeta_\mathsf{x} = x_\mathsf{x} - \frac{1}{g}\begin{bmatrix} 0 \\ 0 \\ 1 \\ \mathrm{d}/\mathrm{d}t \end{bmatrix} q_\mathsf{x}(x)
$$

$$(1.23)$$

to the closed loop system described by (1.14). We next get the state space realization:

$$
\begin{aligned}
\frac{\mathrm{d}}{\mathrm{d}t}\zeta &= \left[\begin{array}{c|c} A_\mathsf{x} & 0 \\ \hline 0 & A_\mathsf{z} \end{array}\right]\zeta + \left[\begin{array}{c} B_\mathsf{x} \\ \hline 0 \end{array}\right](\bar{u}_\mathsf{x} + q_{\mathsf{x},*}(x)), \\
\mathsf{x} &= \begin{bmatrix} C_\mathsf{x} & | & 0 \end{bmatrix}\zeta.
\end{aligned}
$$

$$(1.24)$$

Observe that $\zeta = \begin{bmatrix} \zeta_\mathsf{x} & x_\mathsf{z} \end{bmatrix}^T$ and: [3]

$$
\begin{aligned}
q_{\mathsf{x},*}(x) &= -(1/g)\big(\mathrm{d}^2/\mathrm{d}t^2 + a_{\mathsf{x},_1}\,\mathrm{d}/\mathrm{d}t + a_{\mathsf{x},_2}\big)q_\mathsf{x}(x) \\
&= -(a_{\mathsf{x},_1}/g)\big(\mathrm{d}^3\mathsf{x}/\mathrm{d}t^3 + g\,\mathrm{d}\theta/\mathrm{d}t\big) - (a_{\mathsf{x},_2}/g)\big(\mathrm{d}^2\mathsf{x}/\mathrm{d}t^2 + g\,\theta\big) \\
&\quad -(1/g)\Big(\alpha(x) + \big(\beta(x) + g\big)\mathrm{d}^2\theta/\mathrm{d}t^2\Big).
\end{aligned}
$$

$$(1.25)$$

We also get an expression for the transfer function of the state space realization (1.24): [4]

$$
\mathsf{F}_{\zeta_\mathsf{x}}(\mathsf{s}) = C_\mathsf{x}\,(\mathsf{s}I - A_\mathsf{x})^{-1}\,B_\mathsf{x} = -g/\pi_{x_\mathsf{x}}(\mathsf{s}).
$$

$$(1.26)$$

---

[2]In Section 2.2, we formalize this change of variable, and the computations are done in Example 2.

[3]Recall (1.14), (1.15), (1.12), (1.10), (1.11), and: $\mathrm{d}^4\mathsf{x}/\mathrm{d}t^4 = \alpha(x) + \beta(x)\,\mathrm{d}^2\theta/\mathrm{d}t^2$ (see (1.19) and (1.4)).

[4]Recall (1.12), (1.10), (1.11) and (1.13).

8

We can now conclude that with the following control law:

$$\bar{u}_\mathsf{x} = -q_{\mathsf{x},*}(x)$$

system (1.24) is exactly linearized.

1.4. Robust Asymptotic Feedback Linearization

If the computation of (1.25) would not be possible or would be a hard work, we could try to estimate it. Based on the Beard-Jones filter (*cf.* [4, 19, 27, 36, 41]), the following dynamic output feedback is proposed:[5]

$$
\begin{aligned}
\tfrac{\mathrm{d}}{\mathrm{d}t} w_\mathsf{x} &= \left(A_{K_\mathsf{x}} + B_\mathsf{x} G_\mathsf{x}^\ell C_\mathsf{x}\right) w_\mathsf{x} - \left(K_\mathsf{x} + B_\mathsf{x} G_\mathsf{x}^\ell\right)\mathsf{x}, \\
\bar{u}_\mathsf{x} &= G_\mathsf{x}^\ell C_\mathsf{x} w_\mathsf{x} - G_\mathsf{x}^\ell \mathsf{x},
\end{aligned}
\tag{1.27}
$$

where:

$$
A_{K_\mathsf{x}} = A_\mathsf{x} + K_\mathsf{x} C_\mathsf{x}, \quad G_\mathsf{x}^\ell = -\left(C_\mathsf{x} A_{K_\mathsf{x}}^{-1} B_\mathsf{x}\right)^\ell,
$$

$$
K_\mathsf{x} = \begin{bmatrix} a_{\mathsf{x},3} & a_{\mathsf{x},2} & -a_{\mathsf{x},1}\, g & -g \\ a_{\mathsf{x},2} & a_{\mathsf{x},1} & -g & 0 \\ a_{\mathsf{x},1} & 1 & 0 & 0 \\ 1 & 0 & 0 & 0 \end{bmatrix}^{-1} \begin{bmatrix} a_{\mathsf{x},4} - a_{\mathsf{x}_o,4} \\ a_{\mathsf{x},3} - a_{\mathsf{x}_o,3} \\ a_{\mathsf{x},2} - a_{\mathsf{x}_o,2} \\ a_{\mathsf{x},1} - a_{\mathsf{x}_o,1} \end{bmatrix}.
\tag{1.28}
$$

The characteristic polynomial of A_{K_x} is the Hurwitz polynomial:

$$
\pi_{e_\mathsf{x}}(\mathsf{s}) = \det\left(\mathsf{sI} - A_{K_\mathsf{x}}\right) = \mathsf{s}^4 + a_{\mathsf{x}_o,1}\, \mathsf{s}^3 + a_{\mathsf{x}_o,2}\, \mathsf{s}^2 + a_{\mathsf{x}_o,3}\, \mathsf{s} + a_{\mathsf{x}_o,4}.
\tag{1.29}
$$

Introducing the new state variable, $e_\mathsf{x} = w_\mathsf{x} - \zeta_\mathsf{x}$, we get from (1.27) and (1.24), the modified closed loop state description:

$$
\frac{\mathrm{d}}{\mathrm{d}t}\begin{bmatrix} e_\mathsf{x} \\ \zeta_\mathsf{x} \\ x_\mathsf{z} \end{bmatrix} = \underbrace{\left[\begin{array}{c|c|c} A_{K_\mathsf{x}} & 0 & 0 \\ \hline B_\mathsf{x} G_\mathsf{x}^\ell C_\mathsf{x} & A_\mathsf{x} & 0 \\ \hline 0 & 0 & A_\mathsf{z} \end{array}\right]}_{A_{CL}} \begin{bmatrix} e_\mathsf{x} \\ \zeta_\mathsf{x} \\ x_\mathsf{z} \end{bmatrix} + \underbrace{\left[\begin{array}{c} -B_\mathsf{x} \\ \hline B_\mathsf{x} \\ \hline 0 \end{array}\right]}_{B_{CL}} q_{\mathsf{x},*}(x),
$$

$$
\mathsf{x} = \underbrace{\left[\begin{array}{c|c|c} 0 & C_\mathsf{x} & 0 \end{array}\right]}_{C_{CL}} \begin{bmatrix} e_\mathsf{x}^T & \zeta_\mathsf{x}^T & x_\mathsf{z}^T \end{bmatrix}^T.
\tag{1.30}
$$

The transfer functions involved in the state space realization (1.30) are defined here: [6]

$$
\mathsf{F}_{e_\mathsf{x}}(\mathsf{s}) = G_\mathsf{x}^\ell C_\mathsf{x} \left(\mathsf{sI} - A_{K_\mathsf{x}}\right)^{-1} B_\mathsf{x} = a_{\mathsf{x}_o,4}/\pi_{e_\mathsf{x}}(\mathsf{s}),
\tag{1.31}
$$

---

[5]This control law is studied in Section 3, and the computations are done in Example 3.
[6]Recall (1.28), (1.26), (1.29), (1.10), (1.11) and (1.12),

$$\mathsf{F}_{CL}(\mathrm{s}) = C_{CL}\,(\mathrm{sI} - A_{CL})^{-1}\,B_{CL}$$

$$= \begin{bmatrix} 0 & | & C_\mathsf{x} \end{bmatrix} \left[\begin{array}{c|c} (\mathrm{sI} - A_{K_\mathsf{x}})^{-1} & 0 \\ \hline (\mathrm{sI} - A_\mathsf{x})^{-1} B_\mathsf{x} G_\mathsf{x}^\ell C_\mathsf{x} (\mathrm{sI} - A_{K_\mathsf{x}})^{-1} & (\mathrm{sI} - A_\mathsf{x})^{-1} \end{array} \right] \begin{bmatrix} -\mathrm{I} \\ \mathrm{I} \end{bmatrix} B_\mathsf{x}$$

$$\mathsf{F}_{CL}(\mathrm{s}) = \mathsf{F}_{\zeta_\mathsf{x}}(\mathrm{s})\Big(1 - \mathsf{F}_{e_\mathsf{x}}(\mathrm{s})\Big) = -\frac{g}{\pi_{x_\mathsf{x}}(\mathrm{s})}\left(1 - \frac{a_{\mathsf{x}_o,4}}{\pi_{e_\mathsf{x}}(\mathrm{s})}\right) = -g\,\frac{\mathrm{s}\,\bar{\pi}_{w_\mathsf{x}}(\mathrm{s})}{\pi_{x_\mathsf{x}}(\mathrm{s})\,\pi_{e_\mathsf{x}}(\mathrm{s})}\,.$$

$$(1.32)$$

We use above the additional notation $\bar{\pi}_{w_\mathsf{x}}(\mathrm{s}) = \mathrm{s}^3 + a_{\mathsf{x}_o,1}\,\mathrm{s}^2 + a_{\mathsf{x}_o,2}\,\mathrm{s} + a_{\mathsf{x}_o,3}$.

1.5. Discussion

Let us compare the linearization techniques overviewed in Section 1.

1. The Approximated Input-Output Linearization. A natural approach to control nonlinear systems is to use the classical Taylor approximation. This is in fact a very simple approach. However, the corresponding techniques must be applicable in a small neighborhood of a fixed set point. Under some restrictive assumptions related to the external disturbance, this technique can be useful for classes of regulation problems. On the other hand, it is not recommended, for example, in tracking control problems.

2. Exact Input-Output Linearization. The feedback linearization problem is implemented by a (specific) exact state transformation and an application of the feedback control strategy. Notice that this analytic approach requires a complete knowledge of the dynamic model parameters as well as of the corresponding derivatives. However, in many engineering applications, this assumption is not valid. This is true, for example, for problems from the area of industrial robotics, helicopters control, high-performance aircraft control. This situation also occurs in biomedicine and vehicles control (see [37]). To study this problem, many alternative solution approaches have been proposed. We refer to [1, 3, 8, 10, 13, 18, 24] for some well-established and practically implementable feedback linearization techniques in the absence of the exact systems description. In all the works mentioned above, it is required to make some (usually restrictive) additional assumptions related to the main system model. We can mention the so called "communication" system or external dynamics or the complete state measurability assumptions. Evidently, for the general nonlinear systems and also for the control-affine class, these *a priori* assumptions are difficult to verify.

3. Exact Structural Linearization. In Section 1.3, we propose an exact linearization methodology based on a change of variable (*cf.* (1.23)). In Theorem 1 (see Section 2), we explain in details how to find it. Additionally in Lemma 1, we show that this change of variable is supported by the controllability structure of the linearized system (obtained by means of the first order Taylor series based approximation).

Let us compare the exact structural feedback linearization introduced in Section 1.3 and the well known exact input-output linearization, recalled in Section 1.2. In order to enlighten the main idea, consider here $a_{\mathsf{x},4} = a_{\mathsf{x},3} = a_{\mathsf{x},2}$

$= a_{\mathsf{x},1} = 0$. From (1.11), (1.4) and taking into consideration (1.25), we next get the specific control design that corresponds to the proposed linearization

$$u = \bar{u}_{\mathsf{x}}, \ \mathrm{d}^2\theta/\mathrm{d}t^2 = u \ \text{ and } \ q_{\mathsf{x},*}(x) = -\left(1/g\right)\left(\alpha(x) + \left(\beta(x) + g\right)u\right).$$

Additionally, we also obtain the useful relations (recall (1.24), (1.23) and (1.15)):

$$
\begin{aligned}
\left(\alpha(x) + \beta(x)\,u\right) &= -g\left(u + q_{\mathsf{x},*}(x)\right) = -g\left[\begin{array}{cccc} 0 & 0 & 0 & 1 \end{array}\right]^T \mathrm{d}\zeta_{\mathsf{x}}/\mathrm{d}t \\
&= -g\,\mathrm{d}^2\theta/\mathrm{d}t^2 + \mathrm{d}^2q_{\mathsf{x}}/\mathrm{d}t^2 \\
\left(\alpha(x) + \beta(x)\,u\right) &= \mathrm{d}^4\mathsf{x}/\mathrm{d}t^4\,,
\end{aligned}
$$

which can be exactly identified with (1.19).

Note that the above compliance is not a surprising result. Both of the considered procedures are in fact exact linearizations and naturally lead to the same formal result. The formal difference consists in the manner of obtaining this exact linearization. The advantage of the linear representation which we propose is that the nonlinear uncertainty signal q_* can be treated as an additive disturbance signal. Note that this approach constitutes a specific MIMO procedure that pre-stabilizes the given system matrix A.

4. Robust Asymptotic Feedback Linearization . Some important features of the indicated control scheme are emphasized hereafter.

1. Since the nonlinear uncertainty signal q_* obtained in Section 1.3 can be treated as an additive disturbance signal (*cf.* (1.24)), one can then use the well developed linear tools for the disturbances rejections (as for example the Beard-Jones filter (1.27)).

2. For synthesizing the Beard-Jones filter (1.27) the only information one needs is the linear approximation of first variation (1.8) ((1.9)-(1.12) in example).

3. The transfer function (1.32) of the closed-loop state space representation (1.30) constitutes a typical low-pass filter. If the norm of the time derivative of the nonlinear uncertainty signal (1.25) is bounded $\|\mathrm{d}q_{\mathsf{x},*}/\mathrm{d}t\|_\infty \leq \mathcal{S}_\mathcal{R}$ ($q_{\mathsf{x},*}$ has a finite slew rate $\mathcal{S}_\mathcal{R}$), this implies that the steady-state response of (1.30) can be attenuated by increasing the bandwidth of the Beard-Jones filter (1.27). This fact is formally proved in our Lemmas 2 and 3 of Section 3.

4. From consideration of the transfer function (1.31), we can deduce that the remainder generator $\hat{q}_{\mathsf{x},*} = -G_{\mathsf{x}}^\ell C_{\mathsf{x}}e$ of the Beard-Jones filter (1.27) is in fact a reconstructor of the nonlinear uncertainty signal $q_{\mathsf{x},*}$. Therefore the "increment" of the bandwidth of the Beard-Jones filter (1.27) implies that the remainder generator $\hat{q}_{\mathsf{x},*}$ tends to the nonlinear uncertainty signal $q_{\mathsf{x},*}$. The last one implies its attenuation (see the algebraic part of equation (1.27)). Resulting from that, the usual neighborhood stability will be extended (in the sense of an extended neighborhood). This useful property of the proposed control design is formally proved in Corollary 1 (see Section 4).

When using linearization techniques in control, one needs to discuss the conservativeness of the resulting control design approach. This necessity is a simple consequence of the obvious approximating character of the linearization procedures with respect to the initially given dynamics. We discuss these conservativeness [16, 17, 23] aspects after our main theoretical results, namely, after Theorem 2 and Corollary 1, in Section 4.

The remainder of our paper is organized as follows.

In Section 2, we present our main result, namely, the structural feedback linearization technique that we propose. The robust asymptotic extension of the resulting structural feedback linearization is discussed in Section 3. Section 4 is devoted to some theoretical extensions of the main linearization idea proposed in Section 2. The practically oriented example of a PVTOL system is used throughout the paper to illustrate the efficiency of the proposed linearization approach. This culminates in Section 5 that is devoted to the numerical treatment of the PVTOL control. Section 6 summarizes our paper.

2. The Structural Linearization Approach

This section introduces a novel linearization technique for the class of control-affine dynamic systems under consideration. The proposed linearization methodology is based on the given internal structure of the state description of the linearized system characterized by the pair (A, B), with:

$$A \doteq [\partial f / \partial x]_{x=0} \quad \text{and} \quad B \doteq [g]_{x=0} \; .$$

For this reason, we characterize formally the admissible system nonlinearities (see Theorem 1) which are specified by an additional nonlinear perturbation signal q. This characterization is based on a suitable change of variable obtained by means of an auxiliary algebraic structural equation, stated in Lemma 1. The last result makes it possible to map the nonlinear perturbation signal q into a new *nonlinear perturbation signal q_**.

Let us now introduce some additional technical assumptions.

H5. *Structural Assumptions:*

1. *B is monic, that is:* $\ker B = 0$.
2. *The pair (A, B) is controllable.*
3. *The pair (C, A) is observable.*

For the technical proofs of our main theoretic results, we also need some auxiliary results and facts that are collected in the following subsection.

2.1. The Structural Decomposition

Consider the following assumption.

H6. *There exist an uncertainty vector (nonlinear perturbation signal) $q \in \mathscr{Q} \approx \mathbb{R}^{\mu}$ and a linear transformation $S : \mathscr{Q} \to \mathscr{X}$ such that:*

$$f_o(x(t),\, u(t)) = S\, q(x(t),\, u(t))\,. \tag{2.1}$$

Application of the above transformation to the initially given system (1.5), implies the rewritten dynamic model:

$$\begin{array}{rcl} \frac{\mathrm{d}}{\mathrm{d}t}x(t) & = & A\,x(t) + B\,u(t) + S\,q\,, \\ y(t) & = & C\,x(t)\,. \end{array} \tag{2.2}$$

We now prove our next result.

Lemma 1. *Assume that **H**5.1 and **H**5.2 are true. Then:*

1. *the images of A and B span the whole state space $\mathscr{X}$:*

$$\mathrm{Im}\,A + \mathscr{B} = \mathscr{X}\,; \tag{2.3}$$

2. *the linear transformation $\begin{bmatrix} A & B \end{bmatrix} : \mathscr{X} \times \mathscr{U} \to \mathscr{X}$ is right invertible and there exist linear transformations $M : \mathscr{X} \to \mathscr{X}$ and $X : \mathscr{X} \to \mathscr{U}$ such that:*
$$A\,M + B\,X = \mathrm{I}\,; \tag{2.4}$$

3. *there exists a nilpotent solution $M : \mathscr{X} \to \mathscr{X}$ of (2.4) which satisfies:*

$$M^n = 0\,. \tag{2.5}$$

Proof. From **H**5.2, we get: $\mathscr{X} = \langle A \,|\, \mathscr{B} \rangle \subset \mathrm{Im}\,A + \mathscr{B} \subset \mathscr{X}$, which implies: $\mathrm{Im}\,A + \mathscr{B} = \mathscr{X}$. The right invertibility (2.4) of $\begin{bmatrix} A & B \end{bmatrix}$ is a direct consequence of (2.3).

From (2.4), we conclude that $\mathrm{Im}\,(\mathrm{I} - A\,M) \subset \mathrm{Im}\,B = \ker \widehat{N}$, where $\widehat{N} : \mathscr{X} \to \mathscr{X}/\mathscr{B}$ is the canonical projection, thus:

$$\widehat{N}\,A\,M = \widehat{N}\,. \tag{2.6}$$

From **H**5.1, there exists a left inverse $B^{\ell} : \mathscr{X} \to \mathscr{U}$ of $B : \mathscr{U} \to \mathscr{X}$, then once found a matrix M solving (2.6), one solution of (2.4) is:

$$X = B^{\ell}\,(\mathrm{I} - A\,M)\,, \tag{2.7}$$

Using now the celebrated Brunovsky's Theorem [9], one can deduce the existence of bases in $\mathscr{X}$, $\mathscr{U}$ and $\mathscr{X}/\mathscr{B}$ with the property:

$$\widehat{N}\,A = \mathrm{BD}\,\{G_1,\, \ldots,\, G_m\} \quad \text{and} \quad \widehat{N} = \mathrm{BD}\,\{N_1,\, \ldots,\, N_m\}\,, \tag{2.8}$$

Here G_i and N_i are matrices in $\mathbb{R}^{(\kappa_i - 1) \times \kappa_i}$, $i \in \{1, \ldots, m\}$ with the property $\sum_{i=1}^{m} \kappa_i = n$ and:

$$
G_i = \begin{bmatrix} 0 & 1 & 0 & \cdots & 0 & 0 \\ . & . & . & \cdots & . & . \\ 0 & 0 & 0 & \cdots & 0 & 1 \end{bmatrix} \quad \text{and} \quad N_i = \begin{bmatrix} 1 & 0 & \cdots & 0 & 0 & 0 \\ . & . & \cdots & . & . & . \\ 0 & 0 & \cdots & 0 & 1 & 0 \end{bmatrix}. \quad (2.9)
$$

The last relation implies that the matrix M is defined as follows[7]:

$$
M = \text{BD}\left\{ M_{1_{[\kappa_1]}}, \ldots, M_{m_{[\kappa_m]}} \right\}, \quad M_{i_{[\kappa_i]}} = \begin{bmatrix} 0 & 0 & \cdots & 0 & 0 & 0 \\ 1 & 0 & \cdots & 0 & 0 & 0 \\ . & . & \cdots & . & . & . \\ 0 & 0 & \cdots & 0 & 1 & 0 \end{bmatrix} \in \mathbb{R}^{\kappa_i \times \kappa_i},
$$

$$(2.10)$$

where $i \in \{1, \ldots, m\}$. It satisfies conditions (2.4) and (2.5). The proof is completed. $\qquad \square$

We are now ready to present our first main result. For a better readability, this result is organized in a separated subsection.

2.2. The Exact Scheme of the Structural Feedback
    Linearization

The next technical assumption constitutes in fact a future restriction of the dynamic models under consideration. On the other hand, novel control design techniques (in our case a linearization based design) are nowadays associated with some subclasses of general control systems. These particular subclasses are of a specific interest in some areas of the modern Control Engineering and one can treat and "robustify" these systems using some specific properties of the given dynamics. Exactly these properties constitute in fact the systems restrictions mentioned above.

H7. *The subspace $M \operatorname{Im} S$ is contained in the unobservable subspace $\langle \mathscr{K} \mid M \rangle$, namely:*

$$
C M \mathcal{C}_{(M, S)} = 0. \quad (2.11)
$$

Theorem 1. *Given the linear transformations M and X from* Lemma 1, *consider the following change of variable:*

$$
\zeta(t) = x(t) + M \mathcal{C}_{(M, S)} \Psi_n(\mathrm{d}/\mathrm{d}t) q(x(t), u(t)). \quad (2.12)
$$

---

[7] Notice that this matrix M corresponds to the transpose matrix of the Brunovsky canonical form of A.

14

Under Assumptions **H5.1**, **H5.2** and **H7**, the state representation (2.2) is externally equivalent to the following [8]:

$$\begin{aligned}
\tfrac{\mathrm{d}}{\mathrm{d}t}\zeta(t) &= A\,\zeta(t) + B\Big(u(t) + q_*(x(t),\,u(t))\Big), \\
y(t) &= C\zeta(t),
\end{aligned} \tag{2.13}$$

where the nonlinear uncertainty signal q_* is given by:

$$q_*(x(t),\,u(t)) = X\,\mathcal{C}_{(M,\,S)}\,\Psi_n(\mathrm{d}/\mathrm{d}t)\,q(x(t),\,u(t)). \tag{2.14}$$

Proof. From (2.12) and (2.11), we deduce:

$$C\,\zeta(t) = C\,x(t) + C\,M\,\mathcal{C}_{(M,\,S)}\,\Psi_n(\mathrm{d}/\mathrm{d}t)\,q(x(t),\;u(t)) = C\,x(t). \tag{2.15}$$

Applying the change of variable (2.12) to (2.2), and taking into account (2.4) and (2.5), we get:

$$\begin{aligned}
\tfrac{\mathrm{d}}{\mathrm{d}t}\zeta &= A\left(\zeta - M\sum_{i=0}^{n-1}M^i\,S\,\tfrac{\mathrm{d}^i}{\mathrm{d}t^i}q\right) + B\,u + S\,q + M\sum_{i=0}^{n-1}M^i\,S\,\tfrac{\mathrm{d}^{i+1}}{\mathrm{d}t^{i+1}}q \\
&= A\,\zeta + (B\,X - \mathrm{I})\sum_{i=0}^{n-1}M^i\,S\,\tfrac{\mathrm{d}^i}{\mathrm{d}t^i}q + B\,u + S\,q + \sum_{i=1}^{n-1}M^i\,S\,\tfrac{\mathrm{d}^i}{\mathrm{d}t^i}q \\
&= A\,\zeta + B\left(u + X\sum_{i=0}^{n-1}M^i\,S\,\tfrac{\mathrm{d}^i}{\mathrm{d}t^i}q\right).
\end{aligned}$$

The proof is completed. $\qquad\square$

Theorem 1 makes it possible to represent an initially given sophisticated system (2.2) in a specific form which includes an uncertainty signal explicitly determined. We can next use this result and easily define a control strategy that constitutes a feedback linearization. Following this linearization idea, we conclude that the input design:

$$u(t) = -q_*(x(t),\,u(t)), \tag{2.16}$$

for the dynamic system described by (2.13) represents an exact feedback linearizing control.

Hereafter, some conceptual observations are done.

Remark 1. *Roughly speaking, condition (2.11) $M\,\mathrm{Im}\,S \subset \langle \mathscr{K} \mid M \rangle$ implies that $M\,\mathrm{Im}\,S$ is contained in the output decoupling zeros modes [34, 2] of the Brunovsky dual system (cf. (2.10)) $\mathrm{d}\bar{x}/\mathrm{d}t = M\bar{x} + Sq$ and $\bar{y} = C\bar{x}$.*

---

[8]Recall that two representations are called externally equivalent if the corresponding sets of all possible trajectories for the external variables expressed in an *input/output partition* (u, y) are the same [40, 33].

Remark 2. *Condition (2.11) $M \operatorname{Im} S \subset \langle \mathscr{K} \mid M \rangle$ involves that any trajectory $\bar{x}(\cdot)$ of the Brunovsky dual system (cf. (2.10)) $\mathrm{d}\bar{x}/\mathrm{d}t = M\bar{x}$ and $\bar{y} = C\bar{x}$ (such that the initial condition belongs to $M \operatorname{Im} S$) is unobservable.*

Remark 3. *When the pair (A, B) of the system represented by (2.2) is controllable, then the algebraic equation (2.4) is solvable, and thus from Theorem 1, we get the externally equivalent representation (2.13). Notice that q_* is contained in $\operatorname{Im} B$, so its cancelation is not due to any pole-zero cancelation. This fact remains true for the condition: $\operatorname{Im} S \subset \langle A \mid \mathscr{B} \rangle$. In the case that $\operatorname{Im} S \not\subset \langle A \mid \mathscr{B} \rangle$, but $\operatorname{Im} S \subset \mathscr{V}^* + \langle A \mid \mathscr{B} \rangle$, where $\mathscr{V}^*$ is the supremal (A, B)–invariant subspace contained in $\ker C$, $\sup\{\mathscr{V} \subset \ker C \mid \exists F : (A + BF)\mathscr{V} \subset \mathscr{V}\}$, one can then apply a friend state feedback, $F_* \in \{F : \mathscr{X} \to \mathscr{U} \mid (A+BF)\mathscr{V}^* \subset \mathscr{V}^*\}$, for getting [43]: $\Pi \operatorname{Im} S \subset \Pi \langle A + BF_* \mid \mathscr{B} \rangle$, where Π is the canonical projection of $\mathscr{X}$ onto $\mathscr{X}/\mathscr{V}^*$. Hence, Theorem 1 is applied to the system quotiented by $\mathscr{V}^*$. In this quotient procedure could occur a pole-zero cancelation, and one must thus check that there is no a non-Hurwitz zero cancelation.*

The second technical part of our main Example is now presented.

Example 2 (Structural Linearization Approach)**.** *Consider the Academic Example 1 introduced in Section 1 and use the main Theorem 1. Taking into account (1.6)–(1.7) in (1.4) and applying the stabilizing state feedback (1.11), we get (1.14).*

Recall that $\pi_{\mathsf{x}}(\mathrm{s}) = \det(\mathrm{sI} - A_{\mathsf{x}})$ is a Hurwitz polynomial (cf. (1.13)), and notice that (i) $\ker B_{\mathsf{x}} = 0$, (ii) the pair $(A_{\mathsf{x}}, B_{\mathsf{x}})$ is controllable and (iii) the pair $(C_{\mathsf{x}}, A_{\mathsf{x}})$ is observable.

We now consider the solution of equation $A_{\mathsf{x}} M_{\mathsf{x}} + B_{\mathsf{x}} X_{\mathsf{x}} = \mathrm{I}_4$ that can formally be expressed as:

$$
M_{\mathsf{x}} = T_{\mathsf{x}} M_{1_{[4]}} T_{\mathsf{x}}^{-1} = \begin{bmatrix} 0 & 0 & 0 & 0 \\ 1 & 0 & 0 & 0 \\ 0 & -1/g & 0 & 0 \\ 0 & 0 & 1 & 0 \end{bmatrix}, \; X_{\mathsf{x}} = B_{\mathsf{x}}^{\ell} \left(\mathrm{I}_4 - A_{\mathsf{x}} M_{\mathsf{x}} \right) = \begin{bmatrix} -a_{\mathsf{x},3}/g \\ -a_{\mathsf{x},2}/g \\ a_{\mathsf{x},1} \\ 1 \end{bmatrix}^{T}.
$$

$$(2.17)$$

From (2.17) and (1.12) we next deduce:

$$
A_{\mathsf{x}} M_{\mathsf{x}} + B_{\mathsf{x}} X_{\mathsf{x}} = \mathrm{I}_4 \,, \quad M_{\mathsf{x}}^4 = 0 \,, \quad C_{\mathsf{x}} M_{\mathsf{x}} \mathcal{C}_{(M_{\mathsf{x}}, S_{\mathsf{x}})} = 0 \,,
$$
$$
M_{\mathsf{x}} \mathcal{C}_{(M_{\mathsf{x}}, S_{\mathsf{x}})} \Psi_4(\mathrm{d}/\mathrm{d}t) = -(1/g) \begin{bmatrix} 0 & 0 & 1 & \mathrm{d}/\mathrm{d}t \end{bmatrix}^T \,, \qquad (2.18)
$$
$$
X_{\mathsf{x}} \mathcal{C}_{(M_{\mathsf{x}}, S_{\mathsf{x}})} \Psi_4(\tfrac{\mathrm{d}}{\mathrm{d}t}) = -(1/g) \left(\mathrm{d}^2/\mathrm{d}t^2 + a_{\mathsf{x},1} \, \mathrm{d}/\mathrm{d}t + a_{\mathsf{x},2} \right) \,.
$$

Moreover, from (2.18), (2.12) and (2.14), it follows that the change of variable $\zeta_{\mathsf{x}} = x_{\mathsf{x}} + M_{\mathsf{x}} \mathcal{C}_{(M_{\mathsf{x}}, S_{\mathsf{x}})} \Psi_4(\mathrm{d}/\mathrm{d}t) q_{\mathsf{x}}(x)$ has the form (1.23) and that the nonlinear uncertainty signal $q_{\mathsf{x},*}(x) = X_{\mathsf{x}} \mathcal{C}_{(M_{\mathsf{x}}, S_{\mathsf{x}})} \Psi_4(\tfrac{\mathrm{d}}{\mathrm{d}t}) q_{\mathsf{x}}(x)$ has the form (1.25).

3. Robust Asymptotic Feedback Linearization

Recall that the exact feedback linearization (2.16) usually requires a complete knowledge of the system model. Moreover, one also needs the exact formal expressions of the necessary time derivatives in the given nonlinear perturbation signal $q(x, u)$ (*cf.* (2.14)). On the other hand, the approach that we propose has some evident advantages in comparison with the mentioned classical feedback linearizations. Note that we deal with *a priori* unknown nonlinearities $q_*(x, u)$ that belong to $\mathscr{B}$. In the context of Assumption **H5.3** these unknown nonlinearities can effectively be treated with disturbance rejectors based on standard state observers. Let us now introduce the necessary formal hypothesis.

H8. *The state space description* $\Sigma(A, B, C)$ *(2.2) has no finite invariant zeros at the origin. That formally means:*

$$\operatorname{Im} B \cap A \ker C = 0 \,. \tag{3.1}$$

Assumptions **H5.3** and **H8** make it possible to apply results of [5] and to design a robust disturbance rejection (based on the Beard-Jones filter (*cf.* [4, 19, 27, 36, 41])):

$$\begin{aligned} \tfrac{\mathrm{d}}{\mathrm{d}t} w(t) &= (A + KC)\, w(t) - Ky(t) + Bu(t) \,, \\ \hat{q}_*(t) &= -G^\ell \left(C\, w(t) - y(t) \right) \,, \end{aligned} \tag{3.2}$$

and:

$$u(t) = u_c(t) - \hat{q}_*(t) \,. \tag{3.3}$$

Here $K : \mathscr{Y} \to \mathscr{U}$ is an "output injection" that can be computed as follows:

$$\sigma \left\{ (A + K\, C) \right\} \subset \mathbb{C}^- \,, \tag{3.4}$$

and G^ℓ is a left inverse of the static gain $-C\,(A + KC)^{-1}\, B$. The remainder generator is expressed as:

$$\begin{aligned} \tfrac{\mathrm{d}}{\mathrm{d}t} e(t) &= A_K\, e(t) - B\, q_*(x, u) \,, \\ \hat{q}_*(t) &= -G^\ell\, C\, e(t) \,, \end{aligned} \tag{3.5}$$

where $A_K \doteq (A + KC)$, and $e(t) = w(t) - \zeta(t)$.

When the classic Laplace transform of $q_*(x, u)$ is well-defined, we get:

$$\hat{q}_*(\mathsf{s}) = G^\ell\, \mathsf{F}(\mathsf{s})\, q_*(\mathsf{s}) \,. \tag{3.6}$$

Under the natural boundedness assumptions for $q(x, u)$ with a bandwidth ω_c, we have to synthesize a Hurwitz low-pass filter $\mathsf{F}(\mathsf{s})$ with a corner frequency ω_c. This is with the aims to achieve a robust disturbance in a neighborhood around the equilibrium point $(x, u) = (0, 0)$. We also deduce:

$$\| q_*(\omega) - \hat{q}_*(\omega) \| \le \left\| \left(\mathrm{I} - G^\ell\, \mathsf{F}(\jmath\omega) \right) X\, \mathcal{C}_{(M,\, S)}\, \Psi_n(\jmath\omega) \right\| \, \| q(\omega) \| \,. \tag{3.7}$$

We now study the third technical part of the main illustrative example.

Example 3 (Robust Asymptotic Linearization Approach). *From (1.24), (1.12), (3.2) and (3.3), we deduce the state description (cf. (1.27)):*

$$\begin{aligned}
\tfrac{\mathrm{d}}{\mathrm{d}t}\overline{w}_\mathsf{x} &= \left(\overline{A}_{\overline{K}_\mathsf{x}} + \overline{B}_\mathsf{x}G_\mathsf{x}^\ell\overline{C}_\mathsf{x}\right)\overline{w}_\mathsf{x} - \left(\overline{K}_\mathsf{x} + \overline{B}_\mathsf{x}G_\mathsf{x}^\ell\right)\mathsf{x}, \\
\bar{u}_\mathsf{x} &= G_\mathsf{x}^\ell\,\overline{C}_\mathsf{x}\overline{w}_\mathsf{x} - G_\mathsf{x}^\ell\mathsf{x},
\end{aligned} \tag{3.8}$$

where $\overline{w}_\mathsf{x} = T_{ox}^{-1}w_\mathsf{x}$, $T_{ox} = \begin{bmatrix} a_{\mathsf{x},3} & a_{\mathsf{x},2} & -a_{\mathsf{x},1}\,g & -g \\ a_{\mathsf{x},2} & a_{\mathsf{x},1} & -g & 0 \\ a_{\mathsf{x},1} & 1 & 0 & 0 \\ 1 & 0 & 0 & 0 \end{bmatrix}^{-1}$, $\overline{A}_{\overline{K}_\mathsf{x}} = \overline{A}_\mathsf{x} + \overline{K}_\mathsf{x}\overline{C}_\mathsf{x}$,

$(\overline{A}_\mathsf{x}, \overline{B}_\mathsf{x}, \overline{C}_\mathsf{x}, \overline{K}_\mathsf{x}) = (T_{ox}^{-1}A_\mathsf{x}T_{ox}, T_{ox}^{-1}B_\mathsf{x}, C_\mathsf{x}T_{ox}, T_{ox}^{-1}K_\mathsf{x})$, $G_\mathsf{x}^\ell = -\left(C_\mathsf{x}A_{K_\mathsf{x}}^{-1}B_\mathsf{x}\right)^\ell$

$= -\left(\overline{C}_\mathsf{x}\overline{A}_{\overline{K}_\mathsf{x}}^{-1}\overline{B}_\mathsf{x}\right)^\ell$, *and (cf. (1.28))*

$$\overline{A}_\mathsf{x} = \begin{bmatrix} 0 & 0 & 0 & -a_{\mathsf{x},4} \\ 1 & 0 & 0 & -a_{\mathsf{x},3} \\ 0 & 1 & 0 & -a_{\mathsf{x},2} \\ 0 & 0 & 1 & -a_{\mathsf{x},1} \end{bmatrix}, \quad \overline{B}_\mathsf{x} = \begin{bmatrix} -g \\ 0 \\ 0 \\ 0 \end{bmatrix}, \quad \overline{K}_\mathsf{x} = \begin{bmatrix} a_{\mathsf{x},4} - a_{\mathsf{x}_o,4} \\ a_{\mathsf{x},3} - a_{\mathsf{x}_o,3} \\ a_{\mathsf{x},2} - a_{\mathsf{x}_o,2} \\ a_{\mathsf{x},1} - a_{\mathsf{x}_o,1} \end{bmatrix},$$

$$G_\mathsf{x}^\ell = -\left(\overline{C}_\mathsf{x}\,\overline{A}_{\overline{K}_\mathsf{x}}^{-1}\overline{B}_\mathsf{x}\right)^\ell = -a_{\mathsf{x}_o,4}/g, \quad \overline{C}_\mathsf{x} = \begin{bmatrix} 0 & 0 & 0 & 1 \end{bmatrix}. \tag{3.9}$$

The characteristic polynomial and the corresponding transfer function are expressed as follows (cf. (1.31) and (1.29)):

$$\begin{aligned}
\pi_{e_\mathsf{x}}(\mathsf{s}) &= \det\left(\mathsf{s}I - \overline{A}_{\overline{K}_\mathsf{x}}\right) = \mathsf{s}^4 + a_{\mathsf{x}_o,1}\,\mathsf{s}^3 + a_{\mathsf{x}_o,2}\,\mathsf{s}^2 + a_{\mathsf{x}_o,3}\,\mathsf{s} + a_{\mathsf{x}_o,4}, \\
\mathsf{F}_{e_\mathsf{x}}(\mathsf{s}) &= G_\mathsf{x}^\ell\,\overline{C}_\mathsf{x}\left(\mathsf{s}I - \overline{A}_{\overline{K}_\mathsf{x}}\right)^{-1}\overline{B}_\mathsf{x} = a_{\mathsf{x}_o,4}/\pi_{e_\mathsf{x}}(\mathsf{s}).
\end{aligned} \tag{3.10}$$

The characteristic polynomial, the system zeros polynomial and the transfer function of the Beard-Jones filter (3.8) have the known expressions (recall (1.13)):

$$\begin{aligned}
\pi_{\overline{w}_\mathsf{x}}(\mathsf{s}) &= \det\left(\mathsf{s}I - \left(\overline{A}_{\overline{K}_\mathsf{x}} + \overline{B}_\mathsf{x}G_\mathsf{x}^\ell\overline{C}_\mathsf{x}\right)\right) = \mathsf{s}\,\bar{\pi}_{\overline{w}_\mathsf{x}}(\mathsf{s}), \\
\bar{\pi}_{\overline{w}_\mathsf{x}}(\mathsf{s}) &= \mathsf{s}^3 + a_{\mathsf{x}_o,1}\,\mathsf{s}^2 + a_{\mathsf{x}_o,2}\,\mathsf{s} + a_{\mathsf{x}_o,3},
\end{aligned} \tag{3.11}$$

$$\varphi_{\overline{w}_\mathsf{x}}(\mathsf{s}) = \det\left[\begin{array}{c|c} \mathsf{s}I - \left(\overline{A}_{\overline{K}_\mathsf{x}} + \overline{B}_\mathsf{x}G_\mathsf{x}^\ell\overline{C}_\mathsf{x}\right) & -\left(\overline{K}_\mathsf{x} + \overline{B}_\mathsf{x}G_\mathsf{x}^\ell\right) \\ \hline -G_\mathsf{x}^\ell\overline{C}_\mathsf{x} & -G_\mathsf{x}^\ell \end{array} \right] = -G_\mathsf{x}^\ell\,\pi_{x_\mathsf{x}}(\mathsf{s}), \tag{3.12}$$

$$\mathsf{F}_{\overline{w}_\mathsf{x}}(\mathsf{s}) = \varphi_{\overline{w}_\mathsf{x}}(\mathsf{s})/\pi_{\overline{w}_\mathsf{x}}(\mathsf{s}) = -G_\mathsf{x}^\ell\,\pi_{x_\mathsf{x}}(\mathsf{s})\Big/\left(\mathsf{s}\,\bar{\pi}_{\overline{w}_\mathsf{x}}(\mathsf{s})\right). \tag{3.13}$$

Note that:

$$\mathsf{s}\,\bar{\pi}_{\overline{w}_\mathsf{x}}(\mathsf{s}) + a_{\mathsf{x}_o,4} = \pi_{e_\mathsf{x}}(\mathsf{s}). \tag{3.14}$$

The last equation is of a primary importance because it makes it possible to define the Hurwitz polynomials $\bar{\pi}_{\overline{w}_\mathsf{x}}(\mathsf{s})$ and $\pi_{e_\mathsf{x}}(\mathsf{s})$. In that case, the transfer function of the closed loop system (3.8) and (1.24) has a self-closed form (cf. (1.32)) [9]:

$$\mathsf{F}_{CL}(\mathsf{s}) = \frac{\mathsf{F}_{\zeta_\mathsf{x}}(\mathsf{s})}{1 - \mathsf{F}_{\zeta_\mathsf{x}}(\mathsf{s})\mathsf{F}_{\overline{w}_\mathsf{x}}(\mathsf{s})} = \frac{-g}{\pi_{x_\mathsf{x}}(\mathsf{s})}\frac{\mathsf{s}\,\bar{\pi}_{\overline{w}_\mathsf{x}}(\mathsf{s})}{\left(\mathsf{s}\,\bar{\pi}_{\overline{w}_\mathsf{x}}(\mathsf{s}) + a_{\mathsf{x}_o,4}\right)} = -g\frac{\mathsf{s}\,\bar{\pi}_{\overline{w}_\mathsf{x}}(\mathsf{s})}{\pi_{x_\mathsf{x}}(\mathsf{s})\,\pi_{e_\mathsf{x}}(\mathsf{s})}. \tag{3.15}$$

---

[9] Recall that: $G_\mathsf{x}^\ell = -a_{\mathsf{x}_o,4}/g$; see (3.9).

If $q_{\mathsf{x},*}(x)$ is a bounded signal, its steady-state response tends to zero. If it is a signal with a bounded slew rate, then its steady-state response can be attenuated by increasing the bandwidth $a_{\mathsf{x}_o,4}/a_{\mathsf{x}_o,3}$. These conclusions and the possibility to study the corresponding equivalent representations of the given control-affine dynamic systems are direct consequences of the main Theorem1.

We now consider dynamic systems (2.13), (3.5) and (3.3). The corresponding closed-loop model is expressed as follows (*cf.* (1.30)):

$$
\begin{array}{rcl}
\frac{\mathrm{d}}{\mathrm{d}t}\zeta(t) & = & A\,\zeta(t) + B\left(u_c(t) + \tilde{q}_*(t)\right), \\
\frac{\mathrm{d}}{\mathrm{d}t}e(t) & = & A_K\,e(t) - B\,q_*(x,\,u), \\
\tilde{q}_*(t) & = & q_*(t) + G^\ell\,C\,e(t), \\
y(t) & = & C\,\zeta(t).
\end{array}
\tag{3.16}
$$

The time response of the uncertainty error $\tilde{q}_*(t) = q_*(t) - \hat{q}_*(t)$ has the form:

$$
\begin{aligned}
\tilde{q}_*(t) & = q_*(t) + G^\ell\,C\left(\exp\left(A_K t\right) e(0) - \int_0^t \exp\left(A_K(t-\tau)\right) B\,q_*(\tau)\mathrm{d}\tau\right), \\
& = G^\ell\,C\exp\left(A_K t\right)\tilde{k}_0 - G^\ell\,C\,A_K^{-1}\int_0^t \exp\left(A_K(t-\tau)\right) B\,\frac{\mathrm{d}q_*(\tau)}{\mathrm{d}\tau}\mathrm{d}\tau,
\end{aligned}
\tag{3.17}
$$

where $\tilde{k}_0 = e(0) - A_K^{-1}\,B\,q_*(0)$. The time response of the output in that case can be directly calculated:

$$
y(t) = C\exp\left(At\right)\zeta(0) + C\int_0^t \exp\left(A(t-\tau)\right) B\left(u_c(\tau) + \tilde{q}_*(\tau)\right)\mathrm{d}\tau.
\tag{3.18}
$$

We additionally assume that the uncertainty signal q_* has a finite slew rate $\mathcal{S}_\mathcal{R}$:

H9. $\exists\,\mathcal{S}_\mathcal{R} \in \mathbb{R}^+$ and $\|\mathrm{d}q_*/\mathrm{d}t\|_\infty \leq \mathcal{S}_\mathcal{R}$.

Under the above hypothesis we obtain the next analytic result.

Lemma 2. *Assume that the spectrum σ_K of A_K, has no repeated eigenvalues. Denote by $\bar{\omega}_i$ the modulus of each eigenvalue of σ_K and assume that the elements of σ_K have been re-ordered with $\bar{\omega}_1 \leq \cdots \leq \bar{\omega}_n$. Moreover, let ϱ_i be scale factors of the natural frequencies $\bar{\omega}_i$, namely $\varrho_i = \bar{\omega}_i/\bar{\omega}_1$. There then exist positive constants k_1, k_3 and α_0 such that:*

$$
\|\tilde{q}_*(t)\| \leq k_1\,e^{-\alpha_0 t}\left\|\tilde{k}_0\right\| + (k_3/\alpha_0)\,\mathcal{S}_\mathcal{R}\frac{\varrho_n^{n-1}}{\bar{\omega}_1}.
\tag{3.19}
$$

Moreover, for any positive constant ε_1 there exist a time $t_1 > 0$ and a bandwidth $\bar{\omega}_1 \in \mathbb{R}^+$ with the property:

$$
\|\tilde{q}_*(t)\| \leq \varepsilon_1 \qquad \forall\,t \geq t_1.
\tag{3.20}
$$

If (2.13) is Hurwitz stable, there then exists a positive constant k_4 such that:

$$
\left\|y(t) - \left(C\exp\left(A(t-t_1)\right)\zeta(t_1) + C\int_{t_1}^t \exp\left(A(t-\tau)\right) B\,u_c(\tau)\mathrm{d}\tau\right)\right\| \leq k_4\,\varepsilon_1,
\tag{3.21}
$$

for all $t \geq t_1$.

We next prove Lemma 2.

Proof. Since A_K is assumed to be Hurwitz, there exists k_0 and α_0 such that the norm of the time response of the uncertainty error can be expressed as (see (3.17) and **H**9):

$$
\begin{aligned}
\left\| \tilde{q}_*(t) \right\| & \leq k_1 \mathrm{e}^{-\alpha_0 t} \left\| \tilde{k}_0 \right\| + k_2 \left\| A_K^{-1} \right\| \int_0^t \mathrm{e}^{-\alpha_0(t-\tau)} \left\| \frac{\mathrm{d} q_*(\tau)}{\mathrm{d}\tau} \right\| \mathrm{d}\tau\,, \\
& \leq k_1 \mathrm{e}^{-\alpha_0 t} \left\| \tilde{k}_0 \right\| + (k_2/\alpha_0)\, \mathcal{S}_\mathcal{R} \left\| A_K^{-1} \right\|\,,
\end{aligned}
\tag{3.22}
$$

where $k_1 = k_0 \left\| G^\ell\, C \right\|$ and $k_2 = k_0 \left\| G^\ell\, C \right\| \left\| B \right\|$. From Theorem II.5.10 of [12] we deduce:

$$
\begin{aligned}
\left\| \tilde{q}_*(t) \right\| & \leq k_1 \mathrm{e}^{-\alpha_0 t} \left\| \tilde{k}_0 \right\| + (k_2/\alpha_0)\, \mathcal{S}_\mathcal{R} \frac{\left\| A_K \right\|^{n-1}}{\left| \det A_K \right|}\,, \\
& \leq k_1 \mathrm{e}^{-\alpha_0 t} \left\| \tilde{k}_0 \right\| + (k_2/\alpha_0)\, \mathcal{S}_\mathcal{R} \frac{\left\| A_K \right\|^{n-1}}{\bar{\omega}_1^n}\,, \\
& \leq k_1 \mathrm{e}^{-\alpha_0 t} \left\| \tilde{k}_0 \right\| + (k_3/\alpha_0)\, \mathcal{S}_\mathcal{R} \frac{\varrho_n^{n-1}}{\bar{\omega}_1}\,.
\end{aligned}
\tag{3.23}
$$

This fact proves (3.19).

Moreover, (3.20) is a direct consequence of (3.19) and relation (3.21) follows from (3.18) - (3.20), where

$$
k_4 = \left\| C \int_{t_1}^\infty \exp\left(A(t-\tau) \right) B\,\mathrm{d}\tau \right\|.
\tag{3.24}
$$

$\square$

Lemma 2 makes it possible to consider a disturbance with a band limited spectrum and to establish our next result under the next assumption.

H10. *Assume q_* is a band-limited function, namely, there exists a $\mathcal{B}_\mathcal{W} > 0$ such that:*

$$
\mathbf{Q}_*(\omega) = 0\,, \quad \text{for all} \quad |\omega| > \mathcal{B}_\mathcal{W}\,,
$$

with $\mathbf{Q}_*(\omega)$ as a Fourier transform of $q_*(t)$.

Lemma 3. *Under Assumption **H10**, there exists a positive constant k_4 such that:*

$$
\left\| \tilde{q}_*(t) \right\|_\infty \leq k_1 e^{-(\bar{\omega}_1/2)t} \left\| \tilde{k}_0 \right\| + \frac{\mathcal{B}_\mathcal{W}}{\bar{\omega}_1}\, k_4\, \left\| q_*(t) \right\|_\infty\,,
\tag{3.25}
$$

where $\bar{\omega}_1$ is the bandwidth of the Beard-Jones filter (3.2) and $\mathcal{B}_\mathcal{W}$ is the bandwidth of the introduced disturbances signal q_*.

We next prove Lemma 3.

Proof. Using the celebrated Szökefalvi-Nagy's inequality [32], we immediately deduce that:
$$\|q_*\|_\infty = \sqrt{m}\ \sqrt[4]{E_* E_{*1}}\,, \tag{3.26}$$
where E_* and E_{*1} are the energies of q_* and $\mathrm{d}q_*/\mathrm{d}t$. Here:
$$
\begin{aligned}
E_* &= \int_{-\infty}^{\infty} \|q_*(t)\|^2\,\mathrm{d}t \\
&= \frac{1}{2\pi}\int_{-\infty}^{\infty} \|\mathbf{Q}_*(\omega)\|^2\,\mathrm{d}\omega = \frac{1}{2\pi}\int_{-\mathcal{B}_{\mathcal{W}}}^{\mathcal{B}_{\mathcal{W}}} \|\mathbf{Q}_*(\omega)\|^2\,\mathrm{d}\omega < \infty\,, \\
E_{*1} &= \int_{-\infty}^{\infty} \left\|\frac{\mathrm{d}q_*(t)}{\mathrm{d}t}\right\|^2\,\mathrm{d}t = \frac{1}{2\pi}\int_{-\infty}^{\infty} \omega^2\,\|\mathbf{Q}_*(\omega)\|^2\,\mathrm{d}\omega \\
&= \frac{1}{2\pi}\int_{-\mathcal{B}_{\mathcal{W}}}^{\mathcal{B}_{\mathcal{W}}} \omega^2\,\|\mathbf{Q}_*(\omega)\|^2\,\mathrm{d}\omega < \infty\,.
\end{aligned}
\tag{3.27}
$$
Moreover, $\|q_*(t)\| \leq \sqrt{m}\ \sqrt[4]{E\,E_1}$, for all $t \in \mathbb{R}$ and the above equality holds if and only if $q_*(t) = \mathbf{1}\sqrt[4]{E_*\,E_{*1}}\ \mathrm{e}^{-\sqrt{E_{*1}/E_*}|t|}$. From (3.27) we additionally get:
$$E_{*1} \leq \mathcal{B}_{\mathcal{W}}^{\ 2}\,E_*\,. \tag{3.28}$$

In the same manner we also obtain:
$$\|\mathrm{d}q_*/\mathrm{d}t\|_\infty = \sqrt{m}\ \sqrt[4]{E_{*1}\,E_{*2}}\,, \tag{3.29}$$
and finally:
$$E_{*2} \leq \mathcal{B}_{\mathcal{W}}^{\ 2}\,E_{*1}\,, \tag{3.30}$$
where E_{*2} is the the energy of $\mathrm{d}^2q_*/\mathrm{d}t^2$. One can see that for all $q_* \neq 0$ we have:
$$\|\mathrm{d}q_*/\mathrm{d}t\|_\infty \leq \sqrt{m}\ \sqrt[4]{\mathcal{B}_{\mathcal{W}}^{\ 2}\,E_{*1}^2} = \sqrt{\mathcal{B}_{\mathcal{W}}}\ \sqrt[4]{E_{*1}/E_*}\ \|q_*\|_\infty \leq \mathcal{B}_{\mathcal{W}}\ \|q_*\|_\infty\,. \tag{3.31}$$

Therefore (3.22) and (3.31) imply:
$$
\begin{aligned}
\|\tilde{q}_*(t)\| &\leq k_1\mathrm{e}^{-\alpha_0 t}\left\|\tilde{k}_0\right\| + k_2\left\|A_K^{-1}\right\|\int_0^t \mathrm{e}^{-\alpha_0(t-\tau)}\left\|\frac{\mathrm{d}q_*(\tau)}{\mathrm{d}\tau}\right\|\mathrm{d}\tau\,, \\
&\leq k_1\mathrm{e}^{-\alpha_0 t}\left\|\tilde{k}_0\right\| + (k_2/\alpha_0)\left\|A_K^{-1}\right\|\ \mathcal{B}_{\mathcal{W}}\ \|q_*\|_\infty\,.
\end{aligned}
\tag{3.32}
$$

Setting $\alpha_0 = \bar{\omega}_1/2$, we finally deduce (3.25). The proof is completed. $\qquad\square$

Note that it is a usual practice in Electronic Engineering to relate the slew rate $\|\mathrm{d}q_*/\mathrm{d}t\|_\infty$ with the corresponding bandwidth $\mathcal{B}_{\mathcal{W}}$ (as mentioned in (3.31)).

4. Further Extensions of the Neighborhood Stability Concept

We now rewrite the SPFA concept in the case of the particular nonlinear systems of the type (2.13) and prove our next main result.

We assume that the nonlinear perturbation signal $q(x, u)$ satisfies the following two properties (recall (2.4), (2.12) and (2.14)):

P1. $M\,\mathcal{C}_{(M,\,S)}\,\Psi_n(\mathrm{d}/\mathrm{d}t)\,q(x,\,u) = \alpha_M(x)$. Here $\alpha_M(x) : \mathbb{R}^n \to \mathbb{R}^n$ is a continuous differentiable vector field and the matrix $\partial\alpha_M(x)/\partial x\big|_{x=0}$ has no eigenvalue $\lambda = -1$. That means:

$$\|\alpha_M(x_1) - \alpha_M(x_2)\| \le L_M \|x_1 - x_2\|,\ \forall\ x_1, x_2 \in \mathcal{B}_{\rho_1},\ L_M > 0,\ \rho_1 > 0;\quad (4.1)$$

$$\alpha_M(0) = 0;\quad (4.2)$$

$$\det\left(\mathrm{I} + \partial\alpha_M(x)/\partial x\big|_{x=0}\right) \neq 0.\quad (4.3)$$

P2. Let $X\,\mathcal{C}_{(M,\,S)}\,\Psi_n(\mathrm{d}/\mathrm{d}t)\,q(x,\,u) = \alpha_X(x) + \Gamma_X(x)\,u$. Here $\alpha_X(x) : \mathbb{R}^n \to \mathbb{R}^m$ and $\Gamma_X(x) : \mathbb{R}^n \to \mathbb{R}^{m\times m}$ are continuous differentiable vector fields and $\alpha_X(x)$ maps the zero vector into the zero vector. The Lipschitz constant of $\alpha_X(x)$ tends to zero in the neighborhood of the origin and $\Gamma_X(x)$ has no eigenvalue: $\lambda = -1$. Then:

$$\|\alpha_X(x_1) - \alpha_X(x_2)\| \le L_X \|x_1 - x_2\|,\ \forall\ x_1, x_2 \in \mathcal{B}_\rho,$$

$$L_X = \min\left\{\left(\frac{\mathcal{S}_\mathcal{R}}{\rho_0}\right)\rho,\ \mathcal{S}_\mathcal{R}\right\},\ \rho \in \left[0,\ \rho_1\right],\quad (4.4)$$

$$0 < \rho_0 \le \rho_1;$$

$$\alpha_X(0) = 0;\quad (4.5)$$

$$\det\left(\mathrm{I} + \Gamma_X(x)\right) \neq 0\quad \forall\, x \in \mathcal{B}_{\rho_1},\ \rho_1 > 0.\quad (4.6)$$
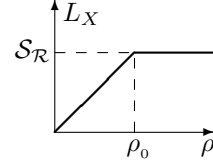
Remark 4. *Under the properties **P1** and **P2**, (2.12) and (2.14) take the following respective forms:*

$$\zeta = x + \alpha_M(x),\quad q_* = \alpha_X(x) + \Gamma_X(x)\,u.\quad (4.7)$$

From (2.12), (2.13), (2.14) and (4.7), we realize that we are obtaining a similar structure as in (1.16): $\zeta = x + \alpha_M(x)$ instead of $\xi = T_{dif}(x)$ and $u + \alpha_X(x) + \Gamma_X(x)\,u$ instead of $\alpha(x) + \beta(x)u$ (recall also Discussion of Section 1.5.3).

Notice also that in (2.2), the state space representation $\Sigma\{A, B, C\}$ is describing the linearized model around the equilibrium point, $(x,\, u) = (0,\, 0)$, so $q(x, u) \to 0$ when $(x,\, u) \to (0,\, 0)$, and thus:[10] $q_*(x, u) \to 0$ when $(x,\, u) \to (0,\, 0)$. This phenomenon is characterized by the shape of the Lipschitz constant L_X (see (4.4)).

---

[10]We are also assuming that the time derivative of q vanish when $(x,\, u) \to (0,\, 0)$.

Based on the above results we are now ready to formulate our second main result.

Theorem 2. *Assume that the nonlinear perturbation signal $q(x, u)$ satisfies properties **P1** and **P2**. Under the conditions of Lemma 2, we have $(x, u) = (0, 0) \in \mathscr{X} \oplus \mathscr{U}$ is an equilibrium point of (2.13). Moreover, there exists a $\rho_2 > 0$ such that:*

$$\mathsf{T}_x^\zeta(x) \doteq x + \alpha_M(x)\,, \tag{4.8}$$

is a diffeomorphism that satisfies:

$$\left\| \mathsf{T}_x^\zeta(x) \right\| \leq (1 + L_M)\, \|x\|\,, \quad \text{for all}\ \ x \in \mathcal{B}_{\rho_1} \cap \mathcal{B}_{\rho_2}\,. \tag{4.9}$$

If in addition:

H11. *For a given $\mu_0 > 1$ there exists $\rho_3 > 0$ such that $\|\alpha_M(x)\| \leq (1 - 1/\mu_0)\, \|x\|$, for all $x \in \cap_{i=1}^{3}\mathcal{B}_{\rho_i}$,*

then, the inverse $\mathsf{T}_\zeta^x : \mathsf{T}_x^\zeta(\mathcal{B}_{\rho_2}) \to \mathcal{B}_{\rho_2}$ satisfies the following condition:

$$\left\| \mathsf{T}_\zeta^x(\zeta) \right\| \leq \mu_0\, \|\zeta\|\,, \quad \text{for all}\ \ \zeta \in \mathsf{T}_x^\zeta \left(\cap_{i=1}^{3}\mathcal{B}_{\rho_i} \right)\,. \tag{4.10}$$

Also, for all non zero ζ belonging to $\mathsf{T}_x^\zeta(\mathcal{B}_\rho)$, where $\rho \in (0,\ \rho_0]$, there holds:

$$\frac{\|q_*(\zeta,\, 0)\|}{\|\zeta\|} \leq \rho \left(\mu_0 \mathcal{S}_\mathcal{R}/\rho_0 \right)\,. \tag{4.11}$$

Furthermore, if A is a Hurwitz matrix, then the autonomous system (2.13) is asymptotically stable in the neighborhood $\mathsf{T}_x^\zeta\left(\mathcal{B}_{\rho_*}\right)$, where:

$$0 < \rho_* < \min \left\{ \rho_0,\, \rho_1,\, \rho_2,\, \rho_3,\, \rho_\# \right\}\,, \tag{4.12}$$

$$\rho_\# = \left(2\, \|B\|\, \overline{\lambda}\, \mu_0\, \mathcal{S}_\mathcal{R}/\rho_0 \right)^{-1}\,, \tag{4.13}$$

and $\overline{\lambda}$ is the maximum eigenvalue of P. Here P is the positive definite matrix solution of the Lyapunov equation $A^T P + PA = -\mathrm{I}$.

We next prove Theorem 2, summarized in Figure 2.

Proof. The proof is done in five steps.

1. *Let us first prove that $(x, u) = (0, 0) \in \mathscr{X} \oplus \mathscr{U}$ is an equilibrium point of (2.13).* Denote $\mathsf{p}_0 \doteq (0,\, 0) \in \mathbb{R}^n \times \mathbb{R}^m$ and define the vector field $\mathsf{f}_\zeta(x,\, u) : \mathbb{R}^n \times \mathbb{R}^m \to \mathbb{R}^n$ by:

$$\mathsf{f}_\zeta(x,\, u) \doteq A\, \zeta(t) + B\Big(u(t) + q_*(x(t),\, u(t)) \Big)\,. \tag{4.14}$$

   Substituting (4.7) into (4.14), we deduce:

$$\mathsf{f}_\zeta(x,\, u) = A\Big(x + \alpha_M(x) \Big) + B\Big(u + \alpha_X(x) + \Gamma_X(x)\, u \Big)\,. \tag{4.15}$$

   Additionally, from (4.2) and (4.5), we also deduce $\mathsf{f}_\zeta(\mathsf{p}_0) = 0$. The last fact implies that p_0 is an equilibrium point of (2.13).
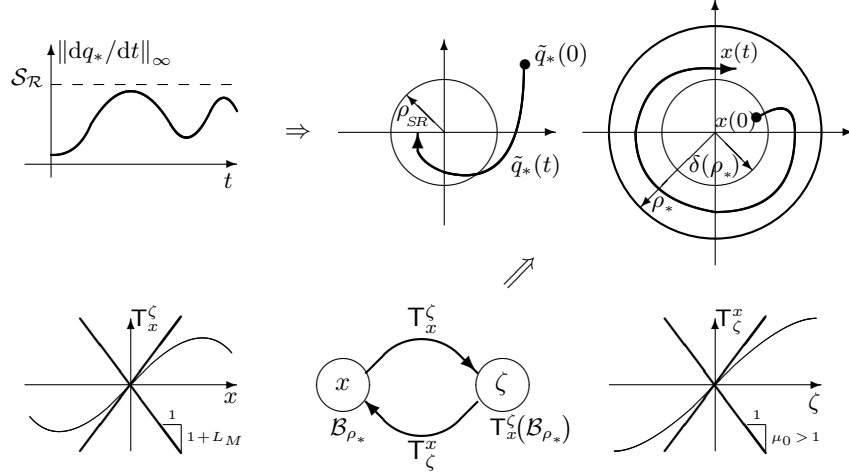
23

Figure 2: Lemma 2: If $\|\mathrm{d}q_*/\mathrm{d}t\|_\infty \leq \mathcal{S}_\mathcal{R}$, then: $\|\tilde{q}_*(t)\|_\infty \leq k_1 \mathrm{e}^{-\alpha_0 t} \left\|\tilde{k}_0\right\| + \rho_{SR}$, where: $\rho_{SR} = (k_3/\alpha_0)\,\mathcal{S}_\mathcal{R}\,(\varrho_n^{n-1}/\bar{\omega}_1)$; $\bar{\omega}_1$ is the bandwidth of (3.2) and $\mathcal{S}_\mathcal{R}$ is the slew rate of q_*: $\|\mathrm{d}q_*/\mathrm{d}t\|_\infty \leq \mathcal{S}_\mathcal{R}$. Theorem 2: For all $x \in \cap_{i=1}^2 \mathcal{B}_{\rho_i}$, $\mathsf{T}_x^\zeta(x) \doteq x + \alpha_M(x)$ is a diffeomorphism satisfying: $\left\|\mathsf{T}_x^\zeta(x)\right\| \leq (1 + L_M)\,\|x\|$. For all $\zeta \in \mathsf{T}_x^\zeta\left(\cap_{i=1}^3 \mathcal{B}_{\rho_i}\right)$, the inverse T_ζ^x satisfies $(\mathsf{T}_\zeta^x(\mathsf{T}_x^\zeta(x)) = x)$: $\left\|\mathsf{T}_\zeta^x(\zeta)\right\| \leq \mu_0\,\|\zeta\|$, $\mu_0 > 1$. If A is Hurwitz, then (2.13) is asymptotically stable in $\mathsf{T}_x^\zeta\left(\mathcal{B}_{\rho_*}\right)$, where: $\rho_* < \min\left\{\rho_0,\,\rho_1,\,\rho_2,\,\rho_3,\,\rho_\#\right\}$, $\rho_\# = \left(2\,\|B\|\,\bar{\lambda}\,\mu_0\,\mathcal{S}_\mathcal{R}/\rho_0\right)^{-1}$.

2. *Let us next prove that (4.9) is satisfied.* Note that from (4.8) and (4.3) it follows that the Jacobian matrix $\partial\mathsf{T}_x^\zeta(x)/\partial x$ is nonsingular at $x = 0$. Recall that the classic Inverse Function Theorem implies that there exists a $\rho_2 > 0$ such that T_x^ζ is a diffeomorphism in $\mathcal{B}_{\rho_2}$ (see *e.g.*, [39], [23], ...). Also, from (4.8), (4.2) and (4.1), we get:

$$\left\|\mathsf{T}_x^\zeta(x)\right\| = \|x + \alpha_M(x)\| \leq (1 + L_M)\,\|x\|\,.$$

3. *Let us now prove that (4.10) is satisfied.* Using (4.8), (4.7) and **H11**, we obtain the series of formal consequences:

$$\left\|\mathsf{T}_\zeta^x(\zeta)\right\| = \left\|\mathsf{T}_\zeta^x\big(x + \alpha_M(x)\big)\right\| = \left\|\mathsf{T}_\zeta^x\big(\mathsf{T}_x^\zeta(x)\big)\right\| = \|x\| = \left\|\mathsf{T}_x^\zeta(x) - \alpha_M(x)\right\|$$
$$= \left\|\zeta - \alpha_M(\mathsf{T}_\zeta^x(\zeta))\right\| \leq \|\zeta\| + (1 - 1/\mu_0)\left\|\mathsf{T}_\zeta^x(\zeta)\right\|.$$

This fact finally implies (4.10).

4. *Let us prove (4.11).* From (4.7), (4.5), (4.4) and (4.10), we get:

$$\frac{\|q_*(\zeta,\,0)\|}{\|\zeta\|} = \frac{\left\|\alpha_X(\mathsf{T}_\zeta^x(\zeta))\right\|}{\|\zeta\|} \leq L_X \frac{\left\|\mathsf{T}_\zeta^x(\zeta)\right\|}{\|\zeta\|} \leq L_X\mu_0 \leq \bar{\rho}\,(\mu_0\mathcal{S}_\mathcal{R}/\rho_0)\,.$$

5. *Let us finally prove the local asymptotic stability of the autonomous system (2.13).* Introduce the Lyapunov function:

$$V(\zeta(t)) = \zeta^T(t)P\zeta(t),$$

24

with P the positive definite matrix solution of the associated Lyapunov equation:

$$A^T P + PA = -\mathrm{I}\,.$$

From (2.13) and (4.11) we finally obtain for all non zero ζ belonging to $\mathsf{T}_x^\zeta\left(\mathcal{B}_{\rho_*}\right)$ (recall (4.12) and (4.13)):

$$
\begin{aligned}
\mathrm{d}V(\zeta(t))/\mathrm{d}t &= \zeta^T(t)\left(A^T P + PA\right)\zeta(t) + 2\left(Bq_*(\zeta(t), 0)\right)^T P\zeta(t)\,, \\
&= -\|\zeta(t)\|^2\left(1 - \frac{2\|B\|\,\|q_*(\zeta, 0)\|\,\|P\|}{\|\zeta(t)\|}\right), \\
&\leq -\|\zeta(t)\|^2\left(1 - 2\,\|B\|\,\rho_*\left(\mu_0\mathcal{S}_\mathcal{R}/\rho_0\right)\overline{\lambda}\right) \\
&= -\|\zeta(t)\|^2\left(1 - \rho_*/\rho_\#\right) < 0\,.
\end{aligned}
$$

The proof is now completed. $\qquad\qquad\square$

The above result is the SPFA version for the case of particular nonlinear systems of the type (2.13) under the structural assumptions of Theorem 2.

Let us discuss shortly the possible conservativeness of the obtained theoretical result [16, 17, 23]. Theorem 2 is proven under specific assumptions for the signal $q(x, u)$, namely, assumptions **P**1 and **P**2. The condition **P**1 constitutes in fact the smoothness of the signal under consideration, the (global) Lipschitz property and the non-singularity hypothesis associated with the second derivative of the signal. Taking into consideration these natural analytic requirements one can characterize **P**1 as a non-restrictive condition. The second assumption related to the signal $q(x, u)$ in Theorem 2 (assumption **P**2) additionally implies a weak dependence on the state variable x at the origin. Evidently, this condition in combination with the assumed linear form of the derivative restricts the universality of the obtained result. However, taking into consideration a wide class of signals that satisfy the above condition **P**1 and **P**2 one can conclude that the developed theory is in some sense conservative for the class of signals under consideration. Since the proof of Theorem 2 uses explicitly the above mentioned assumptions, the "sensitivity" of the obtained robustness theory is a subject for future research.

We next deduce an immediate consequence for the system (2.13) fed back by (3.3) and (3.2), namely for the closed loop system represented by (3.16).

Corollary 1. *Let us consider the autonomous closed loop representation (3.16) satisfying the conditions of Theorem 2 and Lemma 3. Then, the nonlinear uncertainty signals $q_*(x)$ and $\tilde{q}_*(x)$ of the open loop system (2.13) and the closed loop system (3.16) are related as follows:*

$$\|q_*(x)\| \leq \gamma_1\,\|\alpha_x(x)\| + \gamma_2\,\|\tilde{q}_*(x)\|\,, \quad \forall\, x \in \mathcal{B}_{\rho_1}\,, \qquad (4.16)$$

where $\gamma_1 = \sup\limits_{x\in\mathcal{B}_{\rho_1}} \left\|\left(\mathrm{I} + \Gamma_x(x)\right)^{-1}\right\|$ and $\gamma_2 = \sup\limits_{x\in\mathcal{B}_{\rho_1}} \left\|\left(\mathrm{I} + \Gamma_x(x)\right)^{-1}\Gamma_x(x)\right\|$.

Moreover, if the bandwidth $\bar{\omega}_1$ of the Beard-Jones filter (3.2) additionally satisfies:

$$\bar{\omega}_1 > \mathcal{B}_\mathcal{W}\,k_4\,\gamma_2\,, \qquad (4.17)$$

where $\mathcal{B}_\mathcal{W}$ is the bandwidth of q_*, then:

$$\|\tilde{q}_*(\zeta(t))\|_\infty \;\leq\; \frac{k_1\,\bar{\omega}_1/\mathcal{B}_\mathcal{W}}{(\bar{\omega}_1/\mathcal{B}_\mathcal{W} - k_4\,\gamma_2)}\left\|\tilde{k}_0\right\| e^{-\alpha_0 t} \\ +\frac{k_4\,\mu_0\,\gamma_1}{(\bar{\omega}_1/\mathcal{B}_\mathcal{W} - k_4\,\gamma_2)}\,L_X\,\|\zeta(t)\|_\infty\,, \tag{4.18}$$

for all $\zeta \in \mathsf{T}_x^\zeta\left(\cap_{i=1}^3\mathcal{B}_{\rho_i}\right)$.

Furthermore, given $\underline{\rho}_{**}$ and $\overline{\rho}_{**}$ such that $0 < \underline{\rho}_{**} < \overline{\rho}_{**} < \min\{\rho_1,\,\rho_2,\,\rho_3\}$, the time derivative of the Lyapunov function:

$$V(\zeta(t)) = \zeta^T(t)P\zeta(t)\,,$$

where P is the positive definite matrix solution of the associated Lyapunov equation:

$$A^T P + PA = -\mathrm{I}\,,$$

satisfies for all $\zeta(t) \in \mathsf{T}_x^\zeta\left(\mathcal{B}_{\overline{\rho}_{**}}\right) \setminus \mathsf{T}_x^\zeta\left(\mathcal{B}_{\underline{\rho}_{**}}\right)$ and all $t > t_{\#\#}$:

$$\frac{\mathrm{d}}{\mathrm{d}t}V(\zeta(t)) \leq -\left((1+L_M)\underline{\rho}_{**}\right)^2\left(1 - \frac{\rho_{\#\#} - k_4\,\gamma_2}{\bar{\omega}_1/\mathcal{B}_\mathcal{W} - k_4\,\gamma_2}\right)\,, \tag{4.19}$$

where $\overline{\lambda}$ is the maximum eigenvalue of P, α_0 is set to $\bar{\omega}_1/2$, and:

$$\rho_{\#\#} = 4\,\|B\|\,\overline{\lambda}\,(k_4\,\mu_0\,\gamma_1)\,L_X\left(\frac{\overline{\rho}_{**}}{\underline{\rho}_{**}}\right)^2 + k_4\,\gamma_2\,, \tag{4.20}$$

$$t_{\#\#} = \frac{2}{\bar{\omega}_1}\log\left(\frac{(k_1\,\bar{\omega}_1/\mathcal{B}_\mathcal{W})\left\|\tilde{k}_0\right\|}{(k_4\,\mu_0\,\gamma_1)\,L_X\,\overline{\rho}_{**}}\right)\,. \tag{4.21}$$

Finally, if the bandwidth $\bar{\omega}_1$ of the Beard-Jones filter (3.2) satisfies:

$$\bar{\omega}_1 > \mathcal{B}_\mathcal{W}\,\rho_{\#\#}\,, \tag{4.22}$$

then any trajectory $\zeta(t)$ inside $\mathsf{T}_x^\zeta\left(\mathcal{B}_{\overline{\rho}_{**}}\right)$ is attracted towards the neighborhood $\mathsf{T}_x^\zeta\left(\mathcal{B}_{\underline{\rho}_{**}}\right)$, for $t > t_{\#\#}$.

We next prove Corollary 1, summarized in Figure 3.

Proof of Corollary 1. The proof is done in four steps.

1. *Let us first prove that $q_*(x)$ and $\tilde{q}_*(x)$ are related by (4.16). From (2.14), P2, (3.3), (3.5(b)) and (3.16(c)) we deduce:*

$$q_*(x) = \alpha_X(x) + \Gamma_X(x)\Big(\tilde{q}_*(x) - q_*(x)\Big)\,.$$

Then $\big(\mathrm{I} + \Gamma_X(x)\big)q_*(x) = \alpha_X(x) + \Gamma_X(x)\tilde{q}_*(x)$. Relation (4.6) implies

$$q_*(x) = \big(\mathrm{I} + \Gamma_X(x)\big)^{-1}\alpha_X(x) + \big(\mathrm{I} + \Gamma_X(x)\big)^{-1}\Gamma_X(x)\tilde{q}_*(x)\,, \quad \forall\, x \in \mathcal{B}_{\rho_1}\,,$$
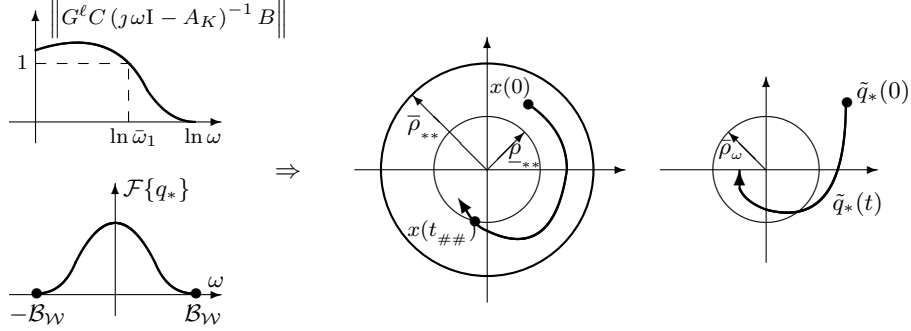
which finally leads to (4.16).

Figure 3: Lemma 3: If $\mathcal{F}\{q_*\} = 0$ for all $|\omega| > \mathcal{B}_\mathcal{W}$, then: $\|\tilde{q}_*(t)\|_\infty \leq k_1 \mathrm{e}^{-(\bar{\omega}_1/2)t} \|\tilde{k}_0\|$ $+ \rho_\omega$, where: $\rho_\omega = (\mathcal{B}_\mathcal{W}/\bar{\omega}_1)k_4\|q_*(t)\|_\infty$; $\bar{\omega}_1$ is the bandwidth of (3.2) and $\mathcal{B}_\mathcal{W}$ is the bandwidth of q_* (see also (3.24)). Corollary 1: If $\bar{\omega}_1 > \mathcal{B}_\mathcal{W} \rho_{\#\#}$, then any $x(t) \in \mathcal{B}_{\bar{\rho}_{**}}$ is attracted towards the neighborhood $\mathcal{B}_{\rho_{**}}$ for $t > t_{\#\#}$. If $\bar{\omega}_1 > \mathcal{B}_\mathcal{W} k_4 \gamma_2$, then: $\|\tilde{q}_*(t)\|_\infty \leq \bar{k}_1 \mathrm{e}^{-\alpha_0 t} \|\tilde{k}_0\| + \bar{\rho}_\omega$, where: $\bar{k}_1 = k_1(\bar{\omega}_1/\mathcal{B}_\mathcal{W})/(\bar{\omega}_1/\mathcal{B}_\mathcal{W} - k_4 \gamma_2)$ and $\bar{\rho}_\omega = (k_4 \mu_0 \gamma_1/(\bar{\omega}_1/\mathcal{B}_\mathcal{W} - k_4 \gamma_2))L_X \|\zeta(t)\|_\infty$.

2. *Let us next prove that $\tilde{q}_*$ satisfies (4.18).* From relations (3.25) and (4.16) we also get:

$$\|\tilde{q}_*(x(t))\|_\infty \leq k_1 \mathrm{e}^{-\alpha_0 t} \|\tilde{k}_0\| + \frac{\mathcal{B}_\mathcal{W}}{\bar{\omega}_1} k_4 \left(\gamma_1 \|\alpha_X(x(t))\|_\infty + \gamma_2 \|\tilde{q}_*(x(t))\|_\infty \right),$$

and:

$$\left(1 - \frac{\mathcal{B}_\mathcal{W}}{\bar{\omega}_1} k_4 \gamma_2\right) \|\tilde{q}_*(x(t))\|_\infty \leq k_1 \mathrm{e}^{-\alpha_0 t} \|\tilde{k}_0\| + \frac{\mathcal{B}_\mathcal{W}}{\bar{\omega}_1} k_4 \gamma_1 \|\alpha_X(x(t))\|_\infty,$$

for all $x \in \cap_{i=1}^3 \mathcal{B}_{\rho_i}$. From (4.17), (4.4), (4.5) and (4.10), we simply obtain (4.18).

3. From (3.16(a)) and (4.18), we obtain that for all $\zeta \in \mathsf{T}_x^\zeta \left(\cap_{i=1}^3 \mathcal{B}_{\rho_i}\right)$:

$$
\begin{aligned}
\frac{\mathrm{d}}{\mathrm{d}t}V(\zeta(t)) = \ & \zeta^T(t)\left(A^T P + PA\right)\zeta(t) + 2\left(B\tilde{q}_*(\zeta(t))\right)^T P\zeta(t), \\
= \ & -\|\zeta(t)\|^2 + 2\left(B\tilde{q}_*(\zeta(t))\right)^T P\zeta(t), \\
\leq \ & -\|\zeta(t)\|^2 + 2\|B\| \,\overline{\lambda}\, \|\tilde{q}_*(\zeta(t))\| \,\|\zeta(t)\|, \\
\leq \ & -\|\zeta(t)\|^2 + 2\|B\| \,\overline{\lambda}\, \left(\frac{k_1 \bar{\omega}_1/\mathcal{B}_\mathcal{W}}{(\bar{\omega}_1/\mathcal{B}_\mathcal{W} - k_4 \gamma_2)}\right) \|\tilde{k}_0\| \,\mathrm{e}^{-\alpha_0 t} \,\|\zeta(t)\|_\infty \\
& +2\|B\| \,\overline{\lambda}\, \left(\frac{k_4 \mu_0 \gamma_1}{(\bar{\omega}_1/\mathcal{B}_\mathcal{W} - k_4 \gamma_2)}\right) L_X \,\|\zeta(t)\|_\infty^2, \\
\leq \ & -\|\zeta(t)\|^2 + \frac{2\|B\| \,\overline{\lambda}}{\bar{\omega}_1/\mathcal{B}_\mathcal{W} - k_4 \gamma_2} \left(\left(k_1 \frac{\bar{\omega}_1}{\mathcal{B}_\mathcal{W}}\right) \|\tilde{k}_0\| \,\mathrm{e}^{-\alpha_0 t}\right. \\
& \left. +(k_4 \mu_0 \gamma_1) L_X \,\|\zeta(t)\|_\infty\right) \|\zeta(t)\|_\infty.
\end{aligned}
$$

27

Setting α_0 to $\bar{\omega}_1/2$ and considering trajectories of ζ inside $\mathsf{T}_x^\zeta\left(\mathcal{B}_{\bar{\rho}_{**}}\right) \setminus$ $\mathsf{T}_x^\zeta\left(\mathcal{B}_{\underline{\rho}_{**}}\right)$, we get (4.19) (recall (4.9)).

4. *Let us finally prove that the trajectories of ζ inside $\mathsf{T}_x^\zeta(\mathcal{B}_{\bar{\rho}_{**}})$ are attracted towards $\mathsf{T}_x^\zeta(\mathcal{B}_{\underline{\rho}_{**}})$.* From (4.19) and (5.21) we get the negativeness of $\mathrm{d}V(\zeta(t))/\mathrm{d}t$.

This completes the proof. $\qquad\square$

For Corollary 1 one can establish similar conservativeness observations as for Theorem 2. We can additionally observe that the (useful) constructive estimation (4.18) is in fact a consequence of the conditions **P**1 and **P**2 and assumption (4.17). In that case the sensitive condition (4.17) has a crucial character for the resulting estimation (4.18).

Also, note that:

1. For the case of the *Approximated Input-Output Linearization*, we can see from Theorem 2 that the stability of system (2.13) (namely system (2.2)) is only guaranteed for the narrow neighborhood ρ_* (*cf.* (4.12) and (4.13)). See Figure 2.

2. For the case of the *Robust Asymptotic Feedback Linearization*, we can realize from Corollary 1 that the stability neighborhood is widely enlarged when the *nonlinear uncertainty estimator* (3.3) and (3.2) is added (*cf.* (3.16)). Indeed, for a given behavioral neighborhood $\mathcal{B}_{\bar{\rho}_{**}}$, a desired attractor neighborhood $\mathcal{B}_{\underline{\rho}_{**}}$ is reached by means of a sufficiently large bandwidth $\bar{\omega}_1$ of the Beard-Jones filter (3.2) (*cf.* (4.20)). Moreover, with the bandwidth filter $\bar{\omega}_1$, we can sufficiently extend the usual linearity neighborhood $\rho_\#$ to $\rho_{\#\#}$, and reduce the regular transitory time $t_{\#\#}$. See Figure 3.

Evidently, the presented results not only establish robustness of the resulting system closed by the proposed control law, but also some structural relations between systems under consideration.

5. Numerical Aspects

We now deal with the last technical part of the Academic Example 1. The final numerical results are obtained using the standard MATLAB$^\circledR$ platform. Consider the following numerical values (obtained from a laboratory prototype):

$$m_T = 0.60\,\mathrm{kg},\ \ J = 0.0032\,\mathrm{kg\,m^2},\ \ L = 0.17\,\mathrm{m},\ \ g = 9.81\,\mathrm{m\,s^{-2}}.$$

The earth axes ($o\mathsf{xyz}$) is located at height $\bar{\mathsf{z}} = 3.00$ [m] with respect to the ground level. Moreover, we examine the following suitable initial conditions: $\mathsf{x}(0) = 0$ [m], $\mathsf{z}(0) = \bar{\mathsf{z}}$, $\mathrm{d}\mathsf{x}(0)/\mathrm{d}t = \mathrm{d}\mathsf{z}(0)/\mathrm{d}t = 0$ [$\mathrm{m\,s^{-1}}$], $\theta(0) = \theta_0$, $\theta_0 = \pi/6$ [rad], $\mathrm{d}\theta(0)/\mathrm{d}t = 0$ [$\mathrm{rad\,s^{-1}}$].

5.1. State feedbacks

The state feedbacks (1.3) and (1.11) are computed using the algebraic Riccati equations:[11] $A_{c_2}^T P_2 + P_2 A_{c_2} - (1/5)P_2 B_z B_z^T P_2 + I_2 = 0$ and $A_{c_4}^T P_4 + P_4 A_{c_4} - (1/5)P_4 B_\times B_\times^T P_4 + I_4 = 0$. Here $F_\times = \begin{bmatrix} -a_{\times,4} & -a_{\times,3} & -a_{\times,2} & -a_{\times,1} \end{bmatrix} = -5 B_\times^T P_4 = \begin{bmatrix} -0.4472 & -1.5814 & -2.5725 & -2.3119 \end{bmatrix}$, and $F_z = \begin{bmatrix} -a_{z,2} & -a_{z,1} \end{bmatrix} = -5 B_z^T P_2 = \begin{bmatrix} -0.4472 & -1.0461 \end{bmatrix}$. The spectra of $A_\times$ and A_z are as follows $\Lambda_\times(s) = \{-0.4162 \pm 0.7387\,\imath, -0.7398 \pm 0.2736\,\imath\}$ and $\Lambda_z(s) = \{-0.5231 \pm 0.4167\,\imath\}$. The spectral radii of $\Lambda_\times(s)$ and $\Lambda_z(s)$ are $\rho_\times = 0.8479$ and $\rho_z = 0.6687$, respectively.

5.2. Beard-Jones filter

Following a root-locus procedure, we get $s\,(s+4.75)(s+4)(s+3.5) + 28.125 = (s+1)^2\,(s^2 + 10.25\,s + 28.125)$. Implementing the Beard-Jones filter 100 times faster than the spectral radius $\rho_\times$ and $\rho_{e_\times} = 100\,\rho_\times$, we obtain $\overline{K}_\times = \begin{bmatrix} -28.125\,\rho_{e_\times}^4 & -66.5\,\rho_{e_\times}^3 & -49.625\,\rho_{e_\times}^2 & -12.25\,\rho_{e_\times} \end{bmatrix}^T$. The initial conditions of (3.8) were set up as (recall (1.23) and (1.20)): $\overline{w}_\times(0) = T_{o\times}^{-1}\,\zeta_\times(0)$, such that:

$$\overline{w}_\times(0) = \begin{bmatrix} a_{\times,3} & a_{\times,2} & -a_{\times,1}\,g & -g \\ a_{\times,2} & a_{\times,1} & -g & 0 \\ a_{\times,1} & 1 & 0 & 0 \\ 1 & 0 & 0 & 0 \end{bmatrix} \begin{bmatrix} \times_0 \\ 0 \\ (1 + a_{z,2}\,z_0/g)\tan(\theta_0) \\ -\left(a_{z,1}\,a_{z,2}\,z_0/g\right)\tan(\theta_0) \end{bmatrix}.$$

5.3. Simulation results

We first have applied to (1.4) the usual exact feedback linearization procedure (1.3) and (1.17), where $\alpha(x)$ and $\beta(x)$ are defined by (1.21). The state ζ is computed based on (1.20). The coefficients of the polynomials $\pi_z(s)$ and $\pi_4(s)$ are determined by the feedbacks F_z and $F_\times$ (see Figure 4). We have also applied to (1.4) the exact structural feedback linearization[12] (1.23) and (1.25). As mentioned above (in Example 2), we have obtained exactly the same time trajectories depicted on Figure 4. We next apply the structural asymptotic feedback linearization (1.3), (1.11) and (3.8) to the given dynamic model (1.2). The coefficients of the polynomials $\pi_z(s)$ and $\pi_{x_\times}(s)$ are determined by the feedbacks F_z and $F_\times$, respectively (see Figure 5). Moreover, $q_{\times,*}(x)$ is defined by (1.25). Notice that the Beard-Jones filter (3.8) quickly tends to the nonlinear uncertainty signal (1.25).

Figure 6 contains an important comparison between the control outputs $u_\times$ obtained in both simulations. We can note that the robust asymptotic feedback linearization scheme is effective in comparison with the usual exact feedback linearization. On the other hand, the asymptotic scheme does not need any nonlinear signal associated with the derivative computation.

---

[11]We have used the LQR technique, with weighting matrices $Q = I_2$ and $R = \rho$ ($\rho = 5$), because one can obtain a good closed-loop behavior by tuning only one parameter, ρ. In [7], we show some experimental results obtained in open field, and we give more details for a good selection of the weight matrix Q.
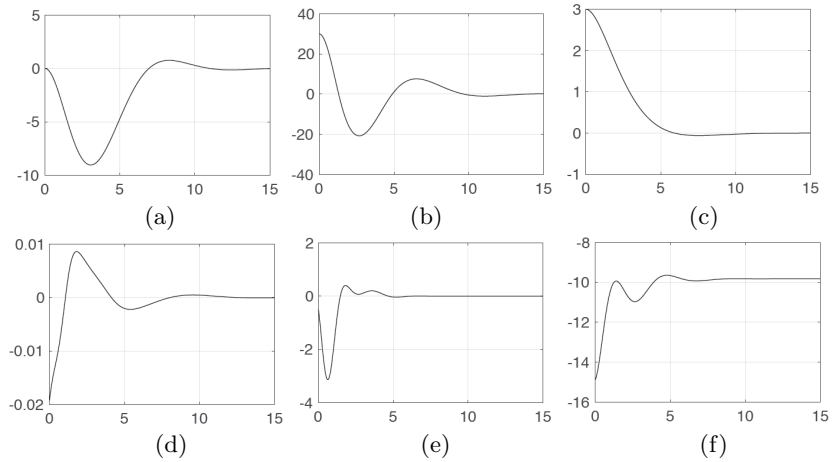
[12]Together with the stabilizing feedback (1.11).

Figure 4: Nonlinear description (1.4) controlled by the usual exact feedback linearization (1.3) and (1.17). (a) x [m], (b) θ [°], (c) z [m], (d) u_x [rad kg m s^{-2}], (e) $\alpha(x)$ [m s^{-4}], (f) $\beta(x)$ [m rad^{-1} s^{-2}],

In this real-world oriented example, one cannot analyze correctly the extension of the linearity neighborhood $\rho_{\#\#}$. We refer to an advanced quadrotor model studied in [6] for this consideration. In the presented example we have obtained a good control performance under the perturbation of $\pi/4$ [rad] with respect to the Euler angles (ϕ, θ, ψ). An interesting and important feature of the robust asymptotic feedback linearization scheme that we propose can be expressed as follows: it takes into account the non-modeled dynamics; see [5] for the theoretic and experimental results. Also, in [7] is presented a detailed synthesis procedure for an experimental quadrotor laboratory prototype, where some simulations are shown, as well as an experimental proof in open field.

The numerical results presented in this section make it clear the advantage of the proposed structural asymptotic feedback linearization technique.
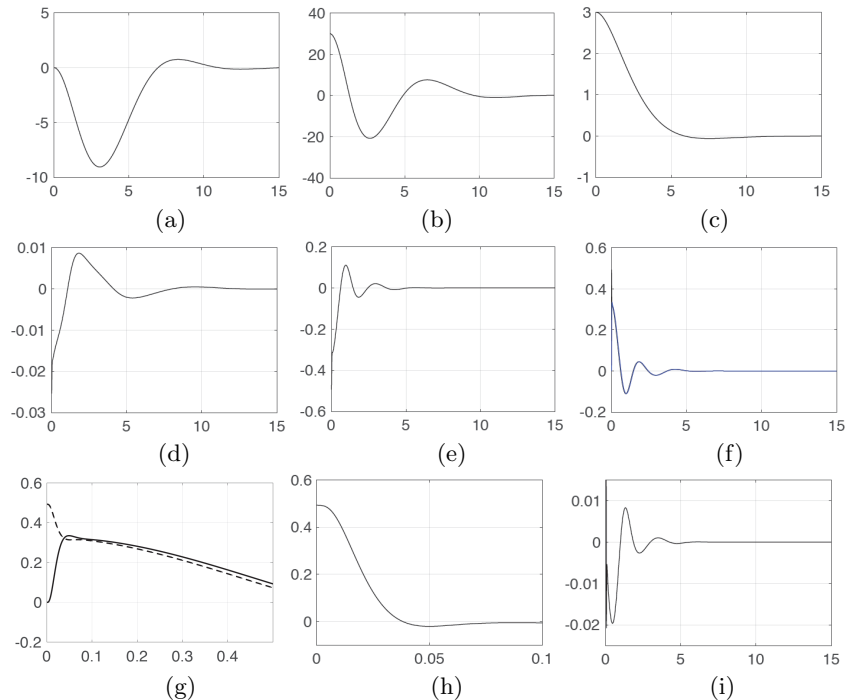
Figure 5: Nonlinear description (1.2) controlled by the robust asymptotic feedback linearization (1.3), (1.11) and (3.8). (a) x [m], (b) θ [°], (c) z [m], (d) $u_\times$ [kg m s^{-2}], (e) $q_{\times,*}(x)$ [s^{-2}], (f) and (g) $q_{\times,*}(x)$ (dash line) vs $\bar{u}_\times$ (solid line) [rad s^{-2}], (h) and (i) $q_{\times,*}(x) - \bar{u}_\times$ [rad s^{-2}].

6. Conclusion

In this paper, we propose a **robust structural feedback linearization** approach based on failure detection techniques. We consider the non-linear affine system (1.1), and describe it equivalently by the specific state space representation (2.2), together with (2.1), (1.7) and (1.6). The newly obtained equivalent system's non-linearities are correspondingly determined by a generic disturbance signal q. The controllability condition for the pair (A, B) makes it possible to treat constructively the derived structural algebraic equation (2.4). The last one defines in fact the necessary change of variable (2.12), that also maps the non-linear disturbance signal q under consideration into a nonlinear uncertainty signal q_*, contained in the image of B; see (2.13) and (2.14).

The proposed equivalent "rewriting" technique makes it finally possible to **design a robust feedback** and to **prove the asymptotic stability** of the initially given dynamic model. The abstract mapping mentioned above involves the basic dynamic representation (2.13). This form implies the possibility of the direct "cancellation" (2.16) of q_*.

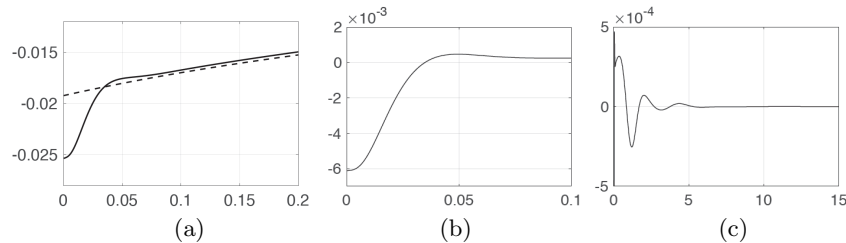If that is not the case, it can be still asymptotically rejected using the Beard-

Figure 6: Comparison of control outputs u_x obtained in both simulations. (a) u_x from Figure 4 (obtained with the exact feedback linearization (1.3) and (1.17); dash line) *vs* u_x from Figure 5 (obtained with the robust asymptotic feedback linearization (1.3), (1.11) and (3.8); solid line) [rad kg m s^{-2}], (b) and (c) Difference of the control signals u_x issued from Figures 4 and 5.

Jones filter (3.2) and (3.3). The main advantage of the developed robust control design is the possibility of the linearity neighborhood extension around the generic equilibrium point 0. Note that the possible uncertainties model is in fact "absorbed" (constructively represented) by q_*. Additionally, we have obtained a useful theoretical fact, summarized in Corollary 1,

"If the bandwidth $\bar{\omega}_1$ of the Beard-Jones filter (3.2) satisfies:

$$\bar{\omega}_1 > \mathcal{B}_\mathcal{W}\,\rho_{\#\#}\,, \tag{5.21}$$

where $\mathcal{B}_\mathcal{W}$ is the bandwidth of q_*, then any trajectory $\zeta(t)$ inside $\mathsf{T}_x^\zeta\left(\mathcal{B}_{\overline{\rho}_{**}}\right)$ is attracted towards the neighborhood $\mathsf{T}_x^\zeta\left(\mathcal{B}_{\underline{\rho}_{**}}\right)$, for $t > t_{\#\#}$",

namely, the high values of the conventional Beard-Jones filter bandwidth of an uncertain signal extend the necessary linearity neighborhood and sufficiently reduce the transitory time.

References

[1] Ahmed S., M.N. Karsiti and G.M. Hassan (2007). Feedback Linearized Strategies for Collaborative Nonholonomic Robots, *International Conference on Control, Automation and Systems*, Seoul Korea, Oct 17-20, pp. 1551–1556.

[2] Aling H. and J.M. Schumacher (1984). A nine-fold canonical decomposition for linear systems, *Int. J. Control*, **39(4)** pp. 779–805.

[3] Back J., K.T.Yu and J.H. Seo (2006). Dynamic observer error linearization, *Automatica*, **42**, pp. 2195–2200.

[4] Beard, R.V. (1971). Failure accommodation in linear systems through self-reorganization. *(PhD thesis, Massachusetts Institute of Technology, 1971.)*

[5] Bonilla M., L.A. Blas, S. Salazar, J.C. Martínez and M. Malabre (2016). A Robust Linear Control Methodology based on Fictitious Failure Rejection. *European Control Conference*, pp. 2596–2601. June 29 - July 1. Aalborg, Denmark.

[6] Blas L.A., Bonilla M., Malabre, M., Azhmyakov, V., Salazar, S. (2017). Structural feedback linearization based on nonlinearities rejection. *20th World Congress*, pp. 945–950. July 9 - 14. Toulouse, France.

[7] Blas L.A., Bonilla M., Salazar, S., Malabre, M., Azhmyakov, V. (2019). Synthesis of a robust linear structural feedback linearization scheme for an experimental quadrotor. *European Control Conference*, 6 pp. June 25-28, Napoli, Italy.

[8] Bortoff S.A. (1997). Approximate State-Feedback Linearization using Spline Functions, *Automatica*, **33(8)**, pp. 1449–1458.

[9] Brunovsky, P. (1970). A classification of linear controllable systems. *Kybernetika* **6(3)**, pp. 173–188.

[10] Cheng D., X. Hu and Y. Wang (2004). Non-regular feedback linearization of nonlinear systems via a normal form algorithm, *Automatica*, **40**, pp. 439–447.

[11] Cook M.V. (2013). **Flight Dynamics Principles. A Linear Systems Approach to Aircraft Stability and Control** *Elsevier Ltd., New York.*

[12] Desoer, C.A. and Vidyasagar, M. (1975). **Feedback Systems: Input-Output Properties.** *Academic Press, New York.*

[13] Kim D.E. and D.C. Lee (2010). Feedback Linearization Control of Three-Phase UPS Inverter Systems, *IEEE Transactions on Industrial Electronics*, **57(3)**, pp. 963–968.

[14] Fritsch O., P. De Monte, M. Buhll and B. Lohmann (2012). Quasi-static feedback linearization for the translational dynamics of a quadrotor helicopter. *2012 American Control Conference (ACC)*, Montréal, Canada, June 27-29, pp. 125–130.

[15] García Carrillo L.R., A.E. Dzul López, R. Lozano and C. Pégard (2013). **Quad Rotorcraft Control. Vision-Based Hovering and Navigation** *Springer-Verlag, London.*

[16] Haddad W.M. and V. Chellaboina (2001). **Dissipativity theory and stability of feedback interconnections for hybrid dynamical 580 systems** *Mathematical Problems in Engineering*, **7(4)**, pp. 299–235.

[17] Haddad W.M., V. Chellaboina and S.G. Nersesov (2014). **Impulsive and Hybrid Dynamical Systems: Stability, Dissipativity and Control** *Princeton University Press*, 2014.

[18] Henmi T., Y. Park, M. Deng and A. Inoue (2010). Stabilization Controller for a Cart-type Inverted Pendulum via a Partial Linearization Method. *International Conference on Modelling, Identification and Control*. Okayama Japan, July 17-19, pp. 248–253.

[19] Isermann, R. (1984). Process fault detection based on modeling and estimation methods-A survey, *Automatica*, **20**, pp. 387–404.

[20] Isidori A. and A. Ruberti (1985). A Relation Between Different Approaches to Input–Output Linearization via Feedback. *Journal of the Franklin Institute*, 320(6), pp. 345–350.

[21] Isidori A. (1989). **Nonlinear Control Systems, An Introduction**, *Springer-Verlag, Berlin.*

[22] Kailath T. (1980). **Linear Systems**, *Prentice Hall, Inc., Englewood Cliffs, New Jersey.*

[23] Khalil H.K. **Nonlinear Systems**, *Macmillan Publishing Company New York* (1992); *Pearson Education, Prentice Hall* (2002).

[24] Komatsu K. and H. Takata (2008). Nonlinear Feedback Control of Stabilization Problem via Formal Linearization Using Taylor Expansion. *International Symposium on Information Theory and its Applications*, 5 pp. Auckland New Zealand, December 7-10.

[25] Kwan-Woong G., K. Hae Dong and K. Chang-Wan (2015). Feedback linearization control of a cardiovascular circulatory simulator. *IEEE Transactions on Control Systems Technology*, 23(5), pp. 1970–1977.

[26] Mahmood A. and K. Yoonsoo (2017). Decentrailized formation flight control of quadcopters using robust feedback linearization. *Journal of the Franklin Institute*, 354(2), pp. 852–871.

[27] Massoumnia M-.A. (1986). A geometric approach to the synthesis of failure detection filters. *IEEE Trans. Automatic Control*, 31(9), pp. 839–846.

[28] Nazrulla S. and H.K. Khalil (2011). Robust Stabilization of Non-Minimum Phase Nonlinear Systems Using Extended High-Gain Observers. *IEEE Transactions on Automatic Control*, **56(4)**, pp. 802–813.

[29] Nijmeijer H. and A.J. Van der Schaft (1990). **Nonlinear dynamical control systems**, *New York : Springer–Verlag.*

[30] Oriolo G., A. De Luca and M. Vendittelli (2002). WMR control via dynamic feedback linearization: design, implementation, and experimental validation. *IEEE Transactions on control systems technology*, **10(6)**, pp. 835–852.

[31] Palli G., C. Melchiorri, T. Wimböck, M. Grebenstein and G. Hirzinger (2007). Feedback linearization and simultaneous stiffness-position control of robots with antagonistic actuated joints. *2007 IEEE International Conference on Robotics and Automation*, Roma, Italy, April 10-14, pp. 4367–4372.

[32] Papoulis A. (1977). **Signal Analysis**, *McGraw-Hill, New York.*

[33] Polderman, J.W., and J.C. Willems (1998). **Introduction to Mathematical Systems Theory: A Behavioral Approach**, *New York: Springer–Verlag.*

[34] Rosenbrock H.H. (1970). **State-Space and Multivariable Theory**, *London: Nelson.*

[35] Slotine, JJ E and Li W. (1991). **Applied Nonlinear Control**, *Prentice Hall NY.*

[36] Saberi, A., Stoorvogel, A.A., Sannuti, P. & Niemann, H.H. (2000). Fundamental problems in fault detection and identification. *International Journal of Robust and Nonlinear Control*, **10**, pp. 1209–1236.

[37] Spong M.W. and M. Vidyasagar (1989). **Robot Dynamics and Control**, *John Wiley & Sons, USA.*

[38] Tang Y. and R.J. Patton (2012). Active FTC for Non-linear Aircraft based on Feedback Linearization and Robust Estimation. *8th IFAC Symposium on Fault Detection, Supervision and Safety of Technical Processes (SAFE-PROCESS)*, Mexico, Mexico City, August 29-31, pp. 210–215.

[39] Vidyasagar M. (1993). **Nonlinear Systems Analysis**, 2nd edition *Prentice-Hall, Inc. New Jersey.*

[40] Willems J.C. (1983). Input–output and state space representations of finite–dimensional linear time–invariant systems, *Linear Algebra and its Applications*, **50**, 581–608.

[41] Willsky, A.S. (1976). A survey of design methods for failure detection in dynamic systems. *Automatica*, **12**, pp. 601–611.

[42] Zhao W. and T.H. Go (2014). Quadcopter formation flight control combining MPC and robust feedback linearization. *Journal of the Franklin Institute*, 351(3), pp. 1335–1355.

[43] Wonham, W.M. (1985). **Linear Multivariable Control: A Geometric Approach**, *New York: Springer-Verlag, 3rd ed*, 1985.